

Reference Energies for Intramolecular Charge-Transfer Excitations

Pierre-François Loos,^{*,†} Massimiliano Comin,[‡] Xavier Blase,^{*,‡} and Denis Jacquemin^{*,¶}

[†]Laboratoire de Chimie et Physique Quantiques, Université de Toulouse, CNRS, UPS, France

[‡]Univ. Grenoble Alpes, CNRS, Inst NEEL, F-38042 Grenoble, France

[¶]Université de Nantes, CNRS, CEISAM UMR 6230, F-44000 Nantes, France

E-mail: loos@irsamc.ups-tlse.fr; xavier.blase@neel.cnrs.fr; Denis.Jacquemin@univ-nantes.fr

Abstract

In the aim of completing our previous efforts devoted to local and Rydberg transitions in organic compounds, we provide a series of highly-accurate vertical transition energies for intramolecular charge-transfer transitions occurring in (π -conjugated) molecular compounds. To this end we apply a composite protocol consisting of linear-response CCSDT excitation energies determined with Dunning’s double- ζ basis set corrected by CC3/CCSDT-3 energies obtained with the corresponding triple- ζ basis. Further basis set corrections (up to *aug-cc-pVQZ*) are obtained at the CCSD and CC2 level. We report 30 transitions obtained in 17 compounds (ABN, aniline, azulene, benzonitrile, benzothiadiazole, DMABN, dimethylaniline, dipeptide, β -dipeptide, hydrogen chloride, nitroaniline, nitrobenzene, nitrodimethylaniline, nitropyridine N-oxide, N-phenylpyrrole, phthalazine, and quinoxaline). These reference values are then used to benchmark a series of wave function (CIS(D), SOPPA, RPA(D), EOM-MP2, CC2, CCSD, CCSD(T)(a)*, CCSDR(3), CCSDT-3, CC3, ADC(2), ADC(3), and ADC(2.5)), the Green’s function-based Bethe-Salpeter equation (BSE) formalism performed on top of the partially self-consistent *evGW* scheme considering two different starting points (BSE/*evGW*@HF and BSE/*evGW*@PBE0), and TD-DFT combined with several exchange-correlation functionals (B3LYP, PBE0, M06-2X, CAM-B3LYP, LC- ω HPBE, ω B97X, ω B97X-D, and M11). It turns out that the CC methods including triples, namely, CCSD(T)(a)*, CCSDR(3), CCSDT-3, and CC3 provide rather small average deviations (≤ 0.10 eV), CC3 emerging as the only chemically accurate approach. ADC(2.5) also performs nicely with a mean absolute error of 0.11 eV for a $O(N^6)$ formal scaling, whereas CC2 and BSE/*evGW*@PBE0 also deliver very satisfying results given their respective $O(N^5)$ and $O(N^4)$ computational scalings. In the TD-DFT context, the best performing functional is ω B97X-D, closely followed by CAM-B3LYP and M06-2X, all providing mean absolute errors around 0.15 eV relative to the theoretical best estimates.

1. CHARGE-TRANSFER EXCITATIONS

Charge-transfer (CT) transitions are key to the working principle of many practical applications of photoactive molecules (OLEDs, photovoltaics, photosynthesis, ion probes, etc). For this reason they have been widely studied, and they are generally regarded as a specific class of excitations, fundamentally different from their more local valence and Rydberg counterparts. While there is no formal definition of CT, chemists generally consider that, in a CT transition, the excitation process transfers a significant fraction of electron density from one molecular fragment, the donor D, to another fragment, the acceptor A. These two fragments can be part of the same molecule (intramolecular CT) or belong to two distinct molecules (intermolecular CT). The CT excitation induces a significant charge shift in going from the ground state (GS) to the excited state (ES), the latter being typically (much) more polar than the former. The reverse situation in which the dipole strongly decreases upon excitation can also be observed (e.g., in betaine 30¹). In other words, CT transitions

are characterized by a large change in dipole moment as well as a small overlap between the starting and final molecular orbitals (MOs), or electron densities, involved in the transition.

From a more theoretical point of view, considering an overall neutral system, one can show that a CT excitation energy behaves, for large enough separation R between the donor and acceptor (the so-called Mulliken limit²) as^{3,4}

$$\Delta E_{\text{CT}} = \text{IP}^{\text{D}} - \text{EA}^{\text{A}} - 1/R, \quad (1)$$

where IP^{D} is the first ionization potential of the donor, EA^{A} is the electron affinity of the acceptor, and $-1/R$ is the electrostatic interaction between the excited electron located on the acceptor fragment and the hole left behind located on the donor fragment. Due to the wrong asymptotic behavior of the kernel associated with (semi-)local exchange-correlation functionals (XCFs), it was quickly recognized that capturing the correct $-1/R$ asymptotic behavior of Eq. (1) is par-

ticularly challenging for time-dependent density-functional theory (TD-DFT).^{5,6} Furthermore, the energy difference between the donor ionization potential (IP^D) and acceptor electron affinity (EA^A) tends to be too small when using Kohn-Sham (KS) orbital energies obtained with semi-local functionals due to the lack of derivative discontinuity into the XCF upon electron addition or removal.⁷ As a result, in its traditional adiabatic formulation, TD-DFT tends to drastically underestimate CT transition energies when combined with local-density approximation (LDA) or generalized-gradient approximation (GGA) XCFs. Some improvements are observed for global hybrid functionals (such as B3LYP⁸⁻¹⁰ and PBE0^{11,12}) that combine a uniform fraction of Hartree-Fock (HF) exchange with a (semi-)local XCF. However, unless 100% of exact exchange is included, a systematic underestimation of CT excitation energies remains due to the relative short-sightedness of global hybrids. Historically, this limitation strongly motivated the development of range-separated hybrids (RSHs)¹³⁻¹⁷ and their optimally-tuned versions^{18,19} which provide a more subtle blend by switching gradually, as a function of the interelectronic distance, from short-range (semi-)local exchange to long-range HF exchange. In such a way, one can combine the best of both worlds by benefiting from the short-range dynamical correlation effects given by DFT as well as key error cancellation between exchange and correlation, while using 100% HF exchange at long range in order to entirely take into account the interaction between the electron and the hole, hence capturing the correct $-1/R$ asymptotic behavior. RSHs are particularly effective at describing CT transitions, but often at the cost of a (slight) overestimation of the transition energies of the corresponding local excitations.²⁰

As an alternative to TD-DFT, one can use the Bethe-Salpeter equation (BSE) formalism²¹⁻²⁸ starting with GW quasiparticle energies²⁹⁻³⁵ (BSE/ GW) as specific formulations of Green's function many-body perturbation theory. By construction, this scheme explicitly includes terms describing the non-local electron-hole interactions, together with an accurate description at the GW level of the ionization potentials and electron affinities, allowing to "naturally" deliver accurate CT energies for a computational cost comparable to TD-DFT.^{28,36-39} The description of the non-local electron-hole interaction thanks to the screened Coulomb potential W allows to consider CT excitations in situations differing from the ideal long-range CT through vacuum, a property central to the study of intramolecular CT or CT in effective dielectric media such as organic semiconductors.⁴⁰⁻⁴⁵ Of course, one can also turn towards wavefunction approaches, and both the second-order algebraic diagrammatic construction [ADC(2)]^{46,47} and approximate second-order coupled-cluster method (CC2)^{48,49} methods are generally regarded as well-suited for accurately describing CT phenomena.

2. CHARGE-TRANSFER METRICS

How does one pinpoint a CT transition? Experimentally, the identification of CT transitions is typically achieved by investigating the absorption spectrum: a strong CT induces a large increase of dipole moment when going from the GS to the ES, which in turn, translates into a broad and structureless

absorption band undergoing significant redshifts when the polarity of the solvent increases (the so-called positive solvatochromism). Theory obviously delivers a complementary view for unveiling CT states. A decade ago, such task was often performed by investigating the topology of the MOs involved in the transition and/or the changes of partial atomic charges following the electronic excitation. Such analyses were certainly successful, but they obviously lacked systematic character. Hence, more quantifiable metrics have been recently developed.

The first we are aware of is the so-called Λ parameter defined by Tozer in 2008.⁵⁰ Λ measures the overlap between the occupied and virtual orbitals involved in a specific transition, and was originally applied by the Tozer group to demonstrate the superiority of RSHs for CT and Rydberg transitions.⁵⁰ In 2011, Le Bahers, Adamo, and Ciofini came up with the d^{CT} metric,⁵¹ which measures the distance between the barycenters of density gain and depletion upon excitation; this model is thus particularly well-acquainted to density-based approaches.^{52,53} Following these two seminal works, many other strategies have been proposed to quantify CTs, such as Guido's Δr ,⁵⁴ which measures the electron-hole distance thanks to an analysis of the charge centroids of the orbitals involved in the excitation, Etienne's ϕ_s which is based on the detachment/attachment matrices,⁵⁵ and the more general approaches developed by Dreuw's group,^{56,57} which allow analyses not only at the TD-DFT level but also with more advanced wavefunction theories such as ADC(2). Several of these metrics have been implemented in well-known quantum chemistry codes and clearly enjoy a strong popularity in the community. In this framework, we specifically highlight the purpose-designed TheoDORE package⁵⁸ encompassing many models for investigating ES topologies.

Although these various metrics do not provide a definite answer to the "what is a CT transition" question, and potentially deliver distinct answers depending on the nature of the underlying (density or wavefunction) description, they nevertheless offer a large panel of options for quantifying the CT strength.

3. LITERATURE SURVEY

To evaluate the performances of specific methods for CT transitions, various sets of reference values have been proposed over the years. Let us describe a selection of some relevant datasets.

In their seminal TD-DFT work,⁵⁰ Peach and coworkers gathered a group of 14 intramolecular CT transitions obtained in three model peptides, N-phenylpyrrole (PP), dimethylamino-benzonitrile (DMABN) and hydrogen chloride (HCl). The reference values were taken from a previous CASPT2^{59,60} work for the peptides,⁶¹ extracted from experiment for DMABN, and determined at the CC2 level for both PP and HCl. The same reference values were used in the following years to assess various DFT approaches.⁶²⁻⁶⁴ However, in 2012, the Tozer group used EOM-CCSD to define new benchmark transition energies for the smallest peptide as well as for both planar and twisted DMABN and PP, in a work encompassing 9 reference CT energies.⁶⁵ The same year, Dev, Agrawal and English compiled a set of 16 CT

transitions in large conjugated dyes,⁶⁶ and they exclusively employed experimental data as reference. In 2015, Heßelmann considered the 10 CASPT2 values obtained for peptides⁶¹ and the 2 EOM-CCSD data determined for PP⁶⁵ as benchmarks for evaluating the performance of non-standard TD-DFT schemes.⁶⁷ All the transitions of the original contribution of Peach and coworkers were re-evaluated in 2019 by Goerigk’s group,⁶⁸ which proposed updated references obtained with CCSDR(3)/cc-pVTZ⁶⁹ (or SCS-CC2)⁷⁰ often using a basis set extrapolation technique similar to the one applied here (*vide infra*). This set was completed by three additional cases, namely *para*-nitro-aniline (pNA) with a reference value obtained with CCSDR(3), the benzene-tetracyanoethylene (B-TCNE) intermolecular complex with a EOM-CCSD(T)⁷¹ reference, and a large dye (so-called DBQ) for which experiment was used as benchmark.⁷² These variations in reference values along the years for Tozer’s original set clearly highlight the appetite of the electronic structure community for high-quality benchmark values, as well as the lack of indisputability for such data even for thoroughly-studied systems.

We wish also to mention that the test set developed by Truhlar and Gagliardi⁷³ contains three CT transitions for pNA [computed at the γ -CR-EOM-CC(2,3)D level],⁷⁴ DMABN (experiment) and B-TCNE (experiment). Two of us considered the same CT transitions to explore the performances of BSE/GW.⁷⁵ In 2018, Gui, Holzer and Klopper,⁷⁶ used a set of seven CT states in pNA, DMABN, PP, HCl and B-TCNE in the similar context. For the first five molecules, they proposed basis set extrapolated CC3/*aug*-cc-pVTZ results, therefore providing again new reference values for those popular systems.

Other sets have been exclusively dedicated to intermolecular CT transitions, which can be viewed as conceptually simpler, as the electron “jumps” from one molecule to another during the CT excitation. Such systems were used already 15 years ago by Truhlar’s group,^{77,78} and have become very popular for benchmarking density- and wavefunction-based methods.^{18,77–85} In 2009, Stein, Kronik and Baer used 13 experimental values measured in CT complexes constituted of an aromatic system interacting with TCNE to assess the performances of their optimally-tuned RSH functional.¹⁸ The same systems were further studied at the BSE level in 2011.³⁶ In 2020, Ottochian and coworkers followed a very similar strategy to benchmark various hybrid and double-hybrid functionals.⁸³ In 2011, Aquino and coworkers employed ADC(2) as reference to benchmark various XCFs for CT occurring in stacked DNA bases.⁷⁹ Similar stacked nucleobases were also studied by Szalay and coworkers in a 2013 work which reports EOM-CCSD(T) data,⁸⁰ in 2014 by Blancafort and Voityuk who obtained CASPT2 energies,⁸¹ and in 2021 by the Matsika group which provided a large set of reference values obtained at the ADC(3)/cc-pVDZ level.⁸⁵

Again, the richness of reference values is obviously both an advantage and a drawback as it is objectively hard to know which work reports the most accurate transition energies. Recently Kozma *et al.* tackled this question by defining 14 accurate intermolecular CT transitions obtained in molecular dimers (e.g., ammonia-fluorine, pyrrole-pyrazine, acetone-

nitromethane, . . .).⁸⁴ In this key work, the reference values are obtained at EOM-CCSDT⁸⁶ or CCSDT-3⁸⁷ levels (depending on the system size) with the cc-pVDZ basis set and several lower-order wavefunction approaches are benchmarked. Interestingly, this study reveals that for intermolecular CT transitions, CCSDT-3 is more accurate than CC3,^{88,89} which is the opposite trends as compared to local and Rydberg transitions.⁹⁰ To the very best of our knowledge, Ref. 84 stands today as the sole work providing reference CT values obtained at a very high level of theory (i.e., EOM-CCSDT).

Our goal here is to propose to the community a list of highly-accurate vertical transition energies for intramolecular CT excitations that can be used as reference to assess the *pros* and *cons* of lower-level models. For instance, there have been recent controversies in the literature regarding the relative accuracy of various double hybrids for CT transitions,^{68,83,91,92} whereas there are significant discrepancies (ca. 0.2 eV) between the recent CC-based theoretical best estimates (TBEs) obtained for pNA, DMABN, and PP by distinct groups,^{68,76} and it is rather difficult to determine the actual origin (basis set, geometry, method, . . .) of these differences.

We do hope that the present (rather large) set can help settling in these uncertainties. Obviously, some systems treated here have been taken from the sets described above, but we have both computed more accurate geometries (*vide infra*) and clearly increased the level of theory employed to define the benchmark TBEs as compared to previous efforts devoted to intramolecular CT. Although these endeavors are well in-line with our recent efforts devoted to local and Rydberg transitions of organic compounds^{93–96} that led to the QUEST database encompassing approximately 500 reference vertical transition energies,^{39,90} it should be noted that the very nature of CT transitions makes the determination of reference values more challenging. Indeed, large density shifts ubiquitous to CT phenomena typically take place in larger compounds than those previously treated. Consequently, (EOM-)CCSDTQ calculations are clearly beyond reach, whereas (EOM-)CCSDT calculations lie at the frontier of today’s possibilities. Beyond completing the QUEST database,^{39,90} we also believe that the present reference values nicely complement the ones recently proposed by the Szalay group for intermolecular CT excitations.⁸⁴ Following the philosophy of the QUEST database, we also wish to avoid any experimental input in order to avoid potential biases and ease theoretical cross comparisons.

4. COMPUTATIONAL METHODS

The investigated systems are displayed in Fig. 1. They include some of the previously described compounds (see Sec. 3), as well as a significant series of new derivatives.

4.1 Geometries

Unless otherwise stated, we use CCSD(T)⁹⁷ or CC3^{88,89} to optimize the ground-state geometry of each compound. These optimizations are carried out with Dunning’s cc-pVTZ basis set using CFOUR2.1⁹⁸ that offers analytical GS nuclear gradients for both methods. As expected, we applied the most advanced approach, CC3, when possible, i.e., for the “smallest” systems investigated. The frozen-core (FC) approximation is enforced during these geometry optimizations. Carte-

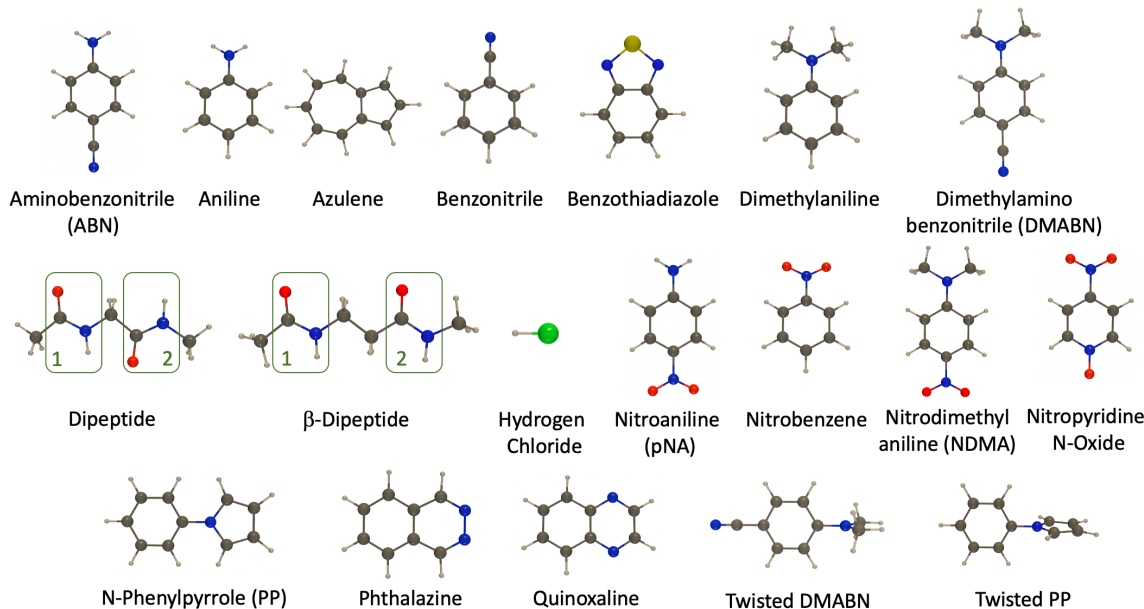


Figure 1: Representation of the investigated derivatives.

sian coordinates and the corresponding optimization method are provided for each compound in the Supporting Information (SI).

Spatial symmetry is enforced during the geometry optimization process which induces some constraints for specific molecules. For example, the C_{2v} point group is enforced for aniline meaning that the amino group is planar. Experimentally, the NH_2 group is puckered, but the symmetry constraint allows for faster calculations as well as an easier ES tracking from one method to another. Of course, such constraints might prevent direct comparisons with experiments, but it is well-known that vertical transition energies have no clear experimental equivalent anyway.⁹⁹

4.2 Basis sets

As further explained below, in a first stage, we perform ES calculations with Dunning’s cc-pVDZ and cc-pVTZ basis sets applying systematically the FC approximation. This allows us to provide TBEs/cc-pVTZ reference values which are subsequently employed to benchmark wavefunction methods. There are several reasons for the choice of cc-pVTZ: i) the same basis set was used in previous benchmark studies devoted to intramolecular CT,^{50,68,100} and ii) the addition of diffuse basis functions would yield lower Rydberg transitions and increase state mixing. This would be detrimental for identifying CT states in some derivatives (e.g., the peptides). We note that Kozma and coworkers went for an even more radical choice (cc-pVDZ) in their recent work,⁸⁴ but we acknowledge that the basis set effects are likely larger for the intramolecular cases treated here. Of course, the absence of diffuse functions in ES calculations is likely to result in (slightly) overestimated transition energies, which is why we also provide estimates with diffuse containing basis sets. This is also justified by the different basis set dependencies of wavefunction- and density-based methods.^{101–103} Therefore, in a second stage, we also perform CCSD calculations^{97,104–107} with *aug-cc-pVTZ*, as well as CC2⁴⁸ cal-

culations with *aug-cc-pVTZ* and *aug-cc-pVQZ* so as to get estimates with larger basis sets. See below for further details.

4.3 Reference calculations

The first stage of the present study deals with the obtention of reference excitation energies for CT excited states. To identify CT transitions in the investigated derivatives, we first determine the lowest 8–20 transitions at the LR-CCSD/cc-pVTZ level with GAUSSIAN 16.¹⁰⁸ We then analyze the nature of the underlying orbitals, and, when possible, compare with literature results. Next, we compute the same ESs at both the ADC(2)/cc-pVTZ^{46,47} and CAM-B3LYP/cc-pVTZ¹⁵ levels of theory using Q-CHEM 5.3¹⁰⁹ and GAUSSIAN 16,¹⁰⁸ respectively. Establishing the correspondence between ESs at different levels of theory is straightforward for the vast majority of the cases. From the CAM-B3LYP calculations, we compute the CT distance, as given by Le Bahers’ model^{51,52} on the basis of the difference between the relaxed TD-DFT density and its GS KS-DFT counterpart. This value is simply labelled d_{CAM}^{CT} below. Likewise, from the ADC(2) data, we compute the electron-hole distance from an analysis of the transition density matrix,^{56,57} labelled r_{ADC}^{eh} in the following. Finally, we also compute, as an estimate of the CT strength, the electron-hole distance determined from the inverse of the expectation value of the direct Coulomb operator over BSE electron-hole eigenstates stemming from the BSE/evGW@HF/cc-pVTZ calculations (see also the SI). These are performed with the FIESTA package.¹¹⁰ These latter values are denoted r_{BSE}^{eh} in the following. Whilst it would certainly be possible to rely on alternative metrics (see Sec. 2), we have selected these three models to have complementary views on the nature of the CT states (DFT *vs* wavefunction *vs* Green’s function, ES density *vs* transition density *vs* Coulomb matrix). As mentioned below, the CT transitions found following such a protocol are usually in agreement with the known literature.

Next, we use CFOUR,⁹⁸ to determine (EOM) CCSDT-

3,^{87,111} CC3,^{88,89} and CCSDT^{86,112–115} transition energies for the states previously identified. For the rather small number of pathological cases, having a LR-CCSD guess is a valuable asset to ease the convergence towards the target ESs. To define our TBEs/cc-pVTZ values, we rely on the following incremental approach

$$\begin{aligned}\Delta E_{\text{TZ}}^{\text{TBE}} &= \Delta E_{\text{cc-pVDZ}}^{\text{CCSDT}} + \left[\Delta E_{\text{cc-pVTZ}}^{\text{CC3}} - \Delta E_{\text{cc-pVDZ}}^{\text{CC3}} \right] \\ &= \Delta E_{\text{cc-pVDZ}}^{\text{CCSDT}} + \Delta \Delta E_{\text{TZ}}^{\text{CC3}},\end{aligned}\quad (2)$$

Such additive scheme is popular in the CC community^{116–122} and similar approaches have been employed in studies involving CT states.^{65,68,76} In Table S5 of the SI, we list the $\Delta \Delta E_{\text{TZ}}$ values obtained with CCSDT-3 and CC3, and their very high degree of similarity is obvious, with a R^2 of 0.99 and a mean absolute deviation between the two sets of data as small as 0.01 eV. In a second step, we have obtained TBEs accounting for diffuse orbitals by applying a similar scheme, that is,

$$\begin{aligned}\Delta E_{\text{ATZ}}^{\text{TBE}} &= \Delta E_{\text{TZ}}^{\text{TBE}} + \left[\Delta E_{\text{aug-cc-pVTZ}}^{\text{CCSD}} - \Delta E_{\text{cc-pVTZ}}^{\text{CCSD(T-3)}} \right] \\ &= \Delta E_{\text{TZ}}^{\text{TBE}} + \Delta \Delta E_{\text{ATZ}}^{\text{CCSD(T-3)}} \\ &= \Delta E_{\text{cc-pVDZ}}^{\text{CCSDT}} + \Delta \Delta E_{\text{TZ}}^{\text{CC3}} + \Delta \Delta E_{\text{ATZ}}^{\text{CCSD(T-3)}}\end{aligned}\quad (3)$$

in which the term $\Delta \Delta E_{\text{ATZ}}$ was typically determined with CCSD, unless CCSDT-3/*aug-cc-pVTZ* calculations were technically feasible. In Table S6 in the SI, we compare the $\Delta \Delta E_{\text{ATZ}}$ values obtained with CC2, CCSD, and CCSDT-3. Whilst the basis set corrections are highly dependent on the considered state and molecule, they are almost unaffected by the level of theory selected, e.g., the absolute difference between the CCSD and CCSDT-3 basis set correction is at most 0.02 eV and 0.01 eV on average. This clearly highlights the transferability of basis set effects between these two wavefunction methods. Eventually, to get even closer to the CBS limit and ease the comparison between wavefunction- and density-based methods, we added additional corrections at the CC2 level, i.e.

$$\begin{aligned}\Delta E_{\text{AQZ}}^{\text{TBE}} &= \Delta E_{\text{ATZ}}^{\text{TBE}} + \left[\Delta E_{\text{aug-cc-pVQZ}}^{\text{CC2}} - \Delta E_{\text{aug-cc-pVTZ}}^{\text{CC2}} \right] \\ &= \Delta E_{\text{ATZ}}^{\text{TBE}} + \Delta \Delta E_{\text{AQZ}}^{\text{CC2}} \\ &= \Delta E_{\text{cc-pVDZ}}^{\text{CCSDT}} + \Delta \Delta E_{\text{TZ}}^{\text{CC3}} + \Delta \Delta E_{\text{ATZ}}^{\text{CCSD(T-3)}} + \Delta \Delta E_{\text{AQZ}}^{\text{CC2}}\end{aligned}\quad (4)$$

The CC2 calculations with both *aug-cc-pVTZ* and *aug-cc-pVQZ* are performed with TURBOMOLE,¹²³ applying the resolution-of-identity (RI) approximation with the corresponding basis sets.¹²⁴ and we have confirmed that the RI approximation has a negligible effect on the present results. As can be seen below, this last correction is marginal for the vast majority of states considered here, so that we do expect that the *aug-cc-pVQZ* basis set provides very accurate estimates for low-lying ESs in organic compounds, and we do not foresee further basis set extension to play a significant role.

4.4 Wavefunction and BSE benchmarks

In the second phase of the present study, we evaluate the performances of several wavefunction- and Green’s function-based approaches using the $\Delta E_{\text{TZ}}^{\text{TBE}}$ values defined in Sec. 4.3 as references. We systematically apply the FC approximation in all these calculations. The following approaches were tested: CIS(D),^{125,126} EOM-MP2,¹²⁷ SOPPA,^{128,129} RPA(D),¹³⁰ CC2,^{48,49} CCSD,⁹⁷ CCSD(T)(a)*,¹³¹ CCSDR(3),⁶⁹ CCSDT-3,^{87,111} CC3,^{88,89} ADC(2),^{46,47} ADC(3),^{47,132,133} ADC(2.5),¹³⁴ and BSE/*GW*.^{21,22,27} The EOM-MP2 and ADC calculations are performed with Q-CHEM 5.2,¹⁰⁹ applying the RI approximation with the cc-pVTZ-RI auxiliary basis set,¹²⁴ and tightening the convergence and integral thresholds. The CIS(D) and CCSD calculations are achieved with GAUSSIAN 16,¹⁰⁸ using default parameters. The SOPPA, RPA(D), CC2 and CCSDR(3) results are obtained with DALTON 2017,¹³⁵ also using default parameters. In the following, we omit the prefixes LR and EOM as both formalisms are known to yield identical excitation energies.^{106,136}

The BSE calculations are performed with the FIESTA package,¹¹⁰ using Coulomb-fitting RI with the cc-pVTZ-RI auxiliary basis set.¹²⁴ The intermediate *GW* quasiparticle energies and screened Coulomb potential *W* are calculated using a partially self-consistent scheme on the eigenvalues (*evGW*) shown in several studies to provide accurate data^{137,138} while significantly removing the dependency on the input KS or HF eigenstates in the final BSE excitation energies.^{76,110,139} Dynamical effects in the *GW* self-energy are treated within an exact contour-deformation approach. For good convergence, all MO energy levels within 10 eV of the HOMO-LUMO gap are explicitly corrected at the *GW* level, lower (higher) states being shifted using the quasiparticle correction obtained for the lowest (highest) explicitly corrected level.¹³⁹ To facilitate the identification of transitions, we first focus on BSE/*evGW* calculations starting from HF eigenstates (BSE/*evGW*@HF), but we next determine the BSE/*evGW* excitation energies obtained starting from PBE0^{11,12} eigenstates (BSE/*evGW*@PBE0), which is a more usual choice in BSE calculations.

4.5 TD-DFT benchmarks

All our TD-DFT calculations have been performed with GAUSSIAN 16,¹⁰⁸ using the *ultrafine* quadrature grid. As the convergence with respect to the basis set size of vertical excitation energies stemming from density-based methods (such as TD-DFT) and wavefunction-based methods tend to significantly differ,^{101–103} we have decided to perform the TD-DFT benchmarks with the *aug-cc-pVQZ* basis set (i.e., using the TBE/*aug-cc-pVQZ* values as references), which is likely large enough to be close to the CBS limit for both families of methods. We have selected the following XCFs to perform our calculations: two global hybrids with rather low exact exchange percentage, B3LYP (20%)^{10,140–142} and PBE0 (25%),^{11,12} one global hybrid with a much larger share of exact exchange, M06-2X (54%),⁷⁸ and five RSHs (CAM-B3LYP,¹⁵ LC- ω HPBE,¹⁴³ ω B97X,¹⁷ ω B97X-D,¹⁴⁴ and M11¹⁴⁵). As mentioned in Sec. 1, it is well recognized that the latter XCFs are better suited for modeling CT transitions. We wish nevertheless to explore the performances

of the global hybrids for “mild” CT as well as the relative performances of the five RSH functionals for various CT strengths.

5. RESULTS AND DISCUSSION

5.1 Reference values

Our reference vertical excitation energies are listed in Table 1, in which we report CCSD, CCSDT-3, CC3, and CCSDT values with two basis sets (cc-pVDZ and cc-pVTZ), as well as literature values and CT strengths evaluated thanks to the three models described in Sec. 4.3. Additional details (oscillator strengths, MO combinations at CCSD level, etc) can be found in the SI. Taking the $r_{\text{ADC}}^{\text{eh}}$ values as reference, one notes a satisfactory agreement with $d_{\text{CAM}}^{\text{CT}}$ for rather small CT (for strong CT, the CAM-B3LYP charge separations appear too small), and a decent match with $r_{\text{BSE}}^{\text{eh}}$ for the cases of large electron-hole separation (for weak CT, the BSE charge separations appear too large). This can be clearly seen in Fig. S1 in the SI. At this stage, we of course highlight that in the case of mild CT character, a change of basis set could induce non-trifling variations of the values given by these CT metrics.

5.1.1 Aminobenzonitrile

Aminobenzonitrile (ABN) is a well-known push-pull molecule, that has been the subject to several previous theoretical studies with wavefunction approaches,^{146,147,175–179} these works typically focussing on the two lowest ESs of local (B_2) and CT (A_1) character. According to the ADC(2) metrics, excitation to this A_1 state induces a charge separation of ca. 1 Å (see Table 1), and there is a perfect match between the CC3 and CCSDT values, whereas CCSDT-3 (CCSD) seem to deliver slightly (significantly) overestimated values. Our TBE/cc-pVTZ, 5.26 eV, perfectly matches the value obtained in the most recent CASPT2 study we are aware of,¹⁷⁸ and is also in quite good agreement with a twenty-year-old STEOM-CCSD estimate (5.13 eV).¹⁴⁷ Those two works used the cc-pVDZ basis set however. In contrast, all previous CASPT2 estimates seem to provide smaller values in the 4.44–5.01 eV range.^{146,175–177} The experimental λ_{max} is located at 4.76 eV in an apolar solvent,¹⁴⁸ a value significantly below our basis set corrected vertical transition energy (5.09 eV), as expected in such comparison.

5.1.2 Aniline

For aniline, the lowest A_1 excited state involves more than one MO pair (see the SI) and has a weak CT character ($d_{\text{CAM}}^{\text{CT}} = 1.02$ Å, $r_{\text{ADC}}^{\text{eh}} = 0.83$ Å, and $r_{\text{BSE}}^{\text{eh}} = 1.91$ Å). Indeed, this state was previously characterized as local in a calculation involving the puckered amine,¹⁵⁰ whereas we enforced the C_{2v} point group in the present calculations. The results listed in Table 1 show a remarkable methodological stability, the CC3, CCSDT-3, and CCSDT values all falling inside a tight 0.04 eV window with the cc-pVDZ basis set, whereas the differences obtained with the triple- ζ basis set are relatively small. Our TBE/cc-pVTZ value, 5.87 eV, is strongly lowered when further basis set corrections are accounted for (5.48 eV). The latter value is in good agreement with the investigation of Worth’s group¹⁴⁹ although we recall that we have enforced C_{2v} symmetry here (which also makes comparisons with experiment difficult).

5.1.3 Azulene

Azulene is a very well-known asymmetric isomer of naphthalene. Its electronic transitions have been investigated at various levels of theory,^{152,153,180,181} likely due to its unusual non-Kasha fluorescence. According to the considered metrics, the second ($2A_1$) and third ($2B_2$) singlet ESs exhibit small CT characters. As can be seen in Table 1, CC3 transition energies are again very close from the CCSDT ones, whereas going from the double- to the triple- ζ basis set decreases the predicted transition energies by roughly -0.10 eV, further basis set extensions yielding even smaller changes. Our TBE is very close to a previous CASPT2/6-31G(d) estimate¹⁵² for the A_1 ES, but is significantly higher than the multi-reference result for the B_2 ES. Both our TBES exceed the experimental 0-0 energies by approximately 0.3–0.4 eV,^{153–155} which is the expected trend.

5.1.4 Benzonitrile

In benzonitrile the two lowest transitions of A_1 and B_2 symmetries do not present any significant CT character (not shown). There is however a higher-lying dark A_2 state corresponding to a CT from the π orbital of the cyano moiety parallel to the main molecular plane towards the highly-delocalized LUMO (see the SI for representation of the MOs) that has a CT nature ($r_{\text{ADC}}^{\text{eh}} = 1.18$ Å). Our TBE/cc-pVTZ for this transition is 7.10 eV, which is likely trustworthy as the CC3 and CCSDT results are much alike with the cc-pVDZ basis set (see Table 1). To the best of our knowledge, this specific transition was not investigated previously, but for a rather old CASPT2 analysis that reports a 7.33 eV value for the lowest A_2 ES.¹⁴⁶

5.1.5 Benzothiadiazole

This bicyclic system, BTD, is an extremely popular acceptor unit in solar cell applications.^{182–184} Surprisingly, while one can find many TD-DFT investigations of large dyes encompassing a BTD moiety, there seems to be no previous wavefunction investigation of this (isolated) building block. Contrasting with the previous molecules, the CCSDT-3 transition energy is closer from the CCSDT value than its CC3 counterpart, though all three methods provide very similar excitation energies. Our TBE/*aug*-cc-pVQZ of 4.28 eV, is 0.76 eV above the experimental 0-0 energy,¹⁵⁶ but such large value is not inconsistent with the large experimental Stokes shift,¹⁸⁵ and the strong theoretical elongation of the N–S bonds in going from the GS to the ES.¹⁸⁶

5.1.6 Dimethylaminobenzonitrile

Dimethylaminobenzonitrile (DMABN) is the prototypical system undergoing twisted intramolecular CT (TICT) and it consequently displays a dual-fluorescence signature strongly dependent on the medium. This process has been the subject of countless investigations,^{62–64,70,146–148,150,157,158,175–177,187–199} and it is clearly not our intent to review in details all these works. Besides its TICT feature, DMABN is undoubtedly one of the most popular dye in CT benchmarks.^{50,65,66,68,73,75,76} However, the present work stands again as the first to propose an estimate of CCSDT quality. Our TBE/*aug*-cc-pVQZ, 4.86 eV, should be rather solid given the agreement between CC3 and CCSDT, and the rather limited basis set effects. This TBE is exactly

Table 1: Reference data for CT ESs. For each state, we provide its symmetry and three CT parameters (in Å, see Sec. 2), as well as the transition energies (in eV) obtained with various wave function methods, the TBE/cc-pVTZ and TBE/aug-cc-pVTZ reference excitation energies, the CC2 correction $\Delta E_{CC2}^{\text{ref}}$, and the corresponding basis-set corrected TBE/aug-cc-pVQZ values. These values are obtained with Eqs. 2 to 4, except otherwise stated. Comparisons with literature are given in the rightmost columns.

Molecule	State	cc-pVTZ			cc-pVDZ			cc-pVTZ			aug-cc-pVTZ			aug-cc-pVQZ			Lit.							
		$d_{\text{CAM}}^{\text{CT}}$	$r_{\text{ADC}}^{\text{eh}}$	$r_{\text{BSE}}^{\text{eh}}$	CCSD	CCSDT-3	CC3	CCSDT	CCSD	CCSDT-3	CC3	TBE	CCSD		TBE		$\Delta E_{\text{AOZ}}^{\text{CC2}}$	TBE	Th.	Th.	Exp.	Exp.		
													5.53	5.43	5.39	5.39							5.39	5.39
Aminobenzonitrile	$2 A_1 (\pi \rightarrow \pi^*)$	1.15	1.01	2.05	5.53	5.43	5.39	5.39	5.41	5.30	5.25	5.26	5.23	5.13	5.09	0.00	5.09	4.98 ^a	5.13 ^b	4.76 ^c				
	$2 A_1 (\pi \rightarrow \pi^*)$	1.02	0.83	1.91	6.16	6.08	6.04	6.05	5.99	5.90	5.86	5.87	5.60	5.53	5.50	-0.02	5.48	5.42 ^d	5.34 ^e	5.39 ^f				
	$2 A_1 (\pi \rightarrow \pi^*)$	1.16	1.06	2.36	4.12	4.01	3.98	3.99	4.02	3.92	3.88	3.89	3.97		3.85	0.00	3.84	3.81 ^g	3.46 ^h	3.56 ⁱ	3.57 ^j			
	$2 B_2 (\pi \rightarrow \pi^*)$	1.02	0.95	2.43	4.89	4.68	4.60	4.62	4.82	4.61	4.52	4.55	4.78		4.50	-0.01	4.49	4.15 ^g	4.13 ^h	4.23 ^k				
Benzonitrile	$1 A_2 (\pi_{\text{CN}} \rightarrow \pi^*)$	1.17	1.18	1.73	7.48	7.31	7.25	7.27	7.33	7.15	7.08	7.10	7.28	7.10	7.05	0.00	7.05	7.37 ^a						
	$1 B_2 (\pi \rightarrow \pi^*)$	1.41	1.24	2.30	4.82	4.59	4.50	4.56	4.63	4.40	4.30	4.37	4.56	4.32	4.29	-0.01	4.28			3.52 ^l				
Benzothiadiazole	$2 A_1 (\pi \rightarrow \pi^*)$	1.48	1.44	2.15	5.20	5.10	5.05	5.06	5.10	4.99	4.93	4.94	5.02		4.86	0.00	4.86	4.90 ^m	4.94 ⁿ	4.57 ^o				
	$1 B_2 (\pi \rightarrow \pi^*)$	1.13	0.98	2.20	4.74	4.63	4.59	4.58	4.66	4.53	4.48	4.47	4.58		4.39	0.00	4.40	4.30 ^p	4.48 ^q	4.30 ^r				
	$2 A_1 (\pi \rightarrow \pi^*)$	1.25	1.22	2.02	5.81	5.73	5.68	5.69	5.68	5.58	5.53	5.54	5.54		5.40	0.00	5.40	5.06 ^p	5.16 ^r	5.16 ^r				
Dipeptide	$7 A'' (n_1 \rightarrow \pi_2^*)$	2.17	3.62	3.35	9.07	8.53	8.28	8.39	8.92	8.31	8.04	8.15				0.00		8.07 ^s	8.33 ^t					
β -Dipetide	$7 A' (\pi_1 \rightarrow \pi_2^*)$	2.36	3.16	3.11	9.13	8.85	8.72	8.77	8.90	8.59		8.51 ^u						7.99 ^s	8.59 ^t					
	$10 A'' (n_1 \rightarrow \pi_2^*)$	2.29	4.35	3.22	9.83	9.32	9.08	9.20	9.58	9.02		8.90 ^u						9.13 ^s	9.08 ^t					
Hydrogen Chloride	$1 \Pi (n \rightarrow \sigma^*)$	1.05	0.95	1.66	8.29	8.24	8.23	8.23	8.18	8.12	8.11	8.10 ^v	7.91	7.85	7.84 ^v		7.88 ^w	7.86 ^x	8.23 ^y					
Nitroaniline	$2 A_1 (\pi \rightarrow \pi^*)$	2.02	2.08	2.27	4.96	4.79	4.70	4.76	4.80	4.61	4.51	4.57	4.63		4.40	-0.01	4.39	4.54 ^t	4.30 ^z					
Nitrobenzene	$2 A_1 (\pi \rightarrow \pi^*)$	1.66	1.51	2.07	6.00	5.84	5.78	5.83	5.77	5.59	5.52	5.57	5.62	5.43	5.41	-0.01	5.39	4.99 ^{aa}	5.27 ^{ab}	4.62 ^{ac}	5.11 ^{ad}			
Nitrodimethylaniline	$2 A_1 (\pi \rightarrow \pi^*)$	2.18	2.41	2.37	4.68	4.51	4.42	4.48	4.53	4.33	4.22	4.28	4.39		4.14	-0.01	4.13			3.89 ^{ae}				
Nitropyridine N-Oxide	$2 A_1 (\pi \rightarrow \pi^*)$	1.70	1.97	2.07	4.60	4.39	4.28		4.46	4.24	4.13	4.24 ^{af}	4.32	4.10	4.10	0.00	4.10	4.32 ^{ag}		3.80 ^{ah}				
N-Phenylpyrrole	$2 B_2 (\pi \rightarrow \pi^*)$	2.11	2.13	2.07	6.02	5.77	5.67	5.70	5.84	5.60	5.50	5.53	5.63		5.32	0.00	5.32	5.52 ^t	5.21 ^{ai}					
	$3 A_1 (\pi \rightarrow \pi^*)$	2.28	3.54	3.54	6.72	6.33	6.17	6.24	6.52	6.14	5.97	6.04	6.34		5.85	0.00	5.86	6.07 ^t	5.69 ^{ai}					
Phthalazine	$1 A_2 (n \rightarrow \pi^*)$	1.11	1.87	2.00	4.24	4.05	3.92	3.95	4.26	4.03	3.89	3.93	4.25	4.01	3.91	0.01	3.91	3.74 ^{aj}	3.68 ^{ak}	3.61 ^{al}	3.01 ^{am}			
	$1 B_1 (n \rightarrow \pi^*)$	1.13	1.87	1.86	4.67	4.49	4.38	4.40	4.64	4.43	4.32	4.34	4.61	4.40	4.31	0.00	4.31	4.20 ^{aj}	4.12 ^{ak}	3.91 ^{al}	3.72 ^{am}			
Quinoxaline	$1 B_2 (\pi \rightarrow \pi^*)$	1.51	1.76	2.42	5.20	4.99	4.90	4.95	5.00	4.79	4.69	4.74	4.91	4.69	4.64	-0.01	4.63	4.45 ^{aj}	4.20 ^{ak}	4.34 ^{al}	3.96 ^{an}			
	$3 A_1 (\pi \rightarrow \pi^*)$	1.12	0.97	2.18	6.13	5.97	5.90	5.89	6.01	5.84	5.76	5.75	5.91	5.75	5.66	-0.01	5.65							
	$2 B_1 (n \rightarrow \pi^*)$	1.21	1.85	2.30	6.94	6.59	6.39	6.46	6.87	6.48	6.26	6.33	6.73	6.36	6.21	0.01	6.22							
Twisted DMABN	$1 A_2 (n \rightarrow \pi^*)$	1.99	2.69	2.64	4.43	4.31	4.23	4.24	4.41	4.25	4.15	4.17	4.35		4.11	0.01	4.12	4.25 ^{ao}						
	$1 B_1 (n \rightarrow \pi^*)$	1.74	2.60	2.17	5.27	5.07	4.95	4.98	5.19	4.95	4.81	4.84	5.09	4.74	4.74	0.01	4.75	5.09 ^{ao}						
Twisted PP	$2 B_2 (\pi \rightarrow \pi^*)$	2.33	3.32	3.51	6.19	5.91	5.79	5.85	6.10	5.80	5.67	5.73	5.95	5.95	5.88	0.00	5.88	5.79 ^{ao}	5.35 ^{ap}					
	$2 A_1 (\pi \rightarrow \pi^*)$	2.38	3.32	2.96	6.37	6.09	5.97	6.03	6.18	5.89	5.76	5.82	6.00	6.00	5.64	0.00	5.65	5.45 ^{ap}						
	$1 A_2 (\pi \rightarrow \pi^*)$	2.32	3.27	3.07	6.41	6.21	6.11	6.14	6.35	6.12	6.01	6.04	6.26	6.26	5.95	0.01	5.95	5.89 ^{ap}						
	$1 B_1 (\pi \rightarrow \pi^*)$	2.37	3.37	3.15	6.78	6.54	6.42	6.46	6.61	6.36	6.24	6.28	6.50	6.50	6.17	0.01	6.17	6.31 ^{ao}						

^aCASPT2/DZP value from Ref. 146; ^bSTEOM-CC/cc-pVDZ value from Ref. 147; ^cExperimental maximum in *n*-heptane from Ref. 148; ^dCR-EOM-CCSD(T)/aug-cc-pVDZ value from Ref. 149; ^eSAC-CI value from Ref. 150; ^f λ_{max} (vapor phase) from Ref. 151; ^gVertical CASPT2/6-31G(d) results from Ref. 152; ^h0-0 DF(T)(BHLLYP)/MRCI/TZVPP values from Ref. 153; ⁱ0-0 energy from fluorescence study of Ref. 154; ^jPhotoelectron spectroscopy from Ref. 153; ^k0-0 energy from the fluorescence spectrum of the jet-cooled derivative in Ref. 155; ^l0-0 energy measured in frozen dichlorobenzene matrix from Ref. 156;

^mMRCIS(8,7)+P/ANO-DZ value from Ref. 157; ⁿADC(3)/cc-pVDZ result from Ref. 158; ^oExperimental λ_{max} (vapor phase) from Ref. 159; ^pCASPT2/6-31G(d,p) values from Ref. 160; ^qCCSDR(3)/aug-cc-pVDZ result from Ref. 161; ^rExperimental λ_{max} (vapor phase) from Ref. 151; ^sCASPT2/DZP value from Ref. 161; ^tCCSDR(3)/cc-pVTZ value (basis set extrapolated for the β -Dipeptide) from Ref. 68; ^uCCSDT-3/cc-pVTZ value corrected by the difference between CCSDT/cc-pVDZ and CCSDT-3/cc-pVDZ energies; ^vFCI/cc-pVTZ value (present paper) and FCI/aug-cc-pVTZ from Ref. 93. For the former basis, the same result is obtained with CCSDTQ/cc-pVTZ; ^wPresent CCSDTQ/aug-cc-pVQZ value; ^xFCI/CBS (no FC) estimate from Ref. 93; ^yCC2/cc-pVTZ value from Ref. 50; ^z γ -CR-EOMCC(2,3)/D(6-31+G(d,p)) value from Ref. 73; ^{aa}CASPT2/IB3LYP result from Ref. 162, the most recent CASPT2 we are aware of reports a similar value of 5.01 eV; ^{ab}ADC(3)/def2-TZVP energy from Ref. 164; ^{ac}EELS on monolayer coverage from Ref. 162; ^{ad}Gas-phase optical absorption maximum from Ref. 165, a similar value of 5.15 eV is reported in the more recent Ref. 166; ^{ae}Experimental gas phase value from Ref. 167; ^{af}CCSDT-3/cc-pVTZ value, see text; ^{ag}CASPT2/aug-cc-pVDZ from Ref. 168 (previously unpublished); ^{ah}Extrapolated gas-phase maximum, see Ref. 168; ^{ai}Ext. CC3/aug-cc-pVDZ results from Ref. 169; ^{aj}CC2/aug-cc-pVDZ results from Ref. 169; ^{ak}CASPT2/cc-pVQZ values from Ref. 170; ^{al}From MCD spectra in *n*-heptane from Ref. 171; ^{am}0-0 energy from Ref. 172; ^{an}0-0 energy in vapor from Ref. 173; ^{ao}Ext. CCSD/aug-cc-pVTZ values from Ref. 65; ^{ap}CASPT2/ANO-DZP values from Ref. 174.

the same as the extrapolated CC3/*aug-cc-pVTZ* result of Ref. 76 and is also close to the ADC(3)/*cc-pVDZ* value given by Mewes and coworkers (4.94 eV).¹⁵⁸ Of course, one can also find other estimates at lower levels of theory, e.g., 4.88 eV with CCSD/*aug-cc-pVDZ*,¹⁹⁹ 4.73 eV with STEOM-CCSD,¹⁴⁷ and 4.90 eV with MRCIS(8,7)+P/ANO-DZ,¹⁵⁷ all three being reasonably close to the current TBE. In contrast, previous CASPT2 estimates of 4.41 eV,¹⁷⁵ 4.51 eV,¹⁴⁶ 4.47 eV,¹⁷⁶ 4.45 eV¹⁷⁷ are all significantly too low.

5.1.7 Dimethylaniline

This derivative was much less investigated than the previous one and we could find only two studies of its excited states involving high-level *ab initio* methods [CASPT2¹⁶⁰ and CCSDR(3)¹⁶¹]. The metrics selected in this work describe the two lowest ESs of this compound as having a small CT character with a charge separation of ca. 1 Å with ADC(2), the CT nature of the A_1 transition being only slightly larger than that of the “local” B_2 excitation. Here again, one notes the usual methodological trends as illustrated by the data gathered in Table 1, with superb agreement between the CC3 and CCSDT estimates, and a limited drop of the transition energies when enlarging the basis set. The basis set corrected TBEs of 4.40 and 5.40 eV are reasonably in line with the literature.^{160,161}

5.1.8 Dipeptide and β -dipeptide

Both of these model compounds were originally characterized at the CASPT2 level by Serrano-Andrés and Fülischer.⁶¹ The smaller derivative is a popular test molecule for CT,^{200,201} and is part of Tozer’s^{50,65} and Goerigk’s⁶⁸ sets. In both systems, these works identified two CT transitions, denoted as $\pi_1 \rightarrow \pi_2^*$ and $n_1 \rightarrow \pi_2^*$, the subscript referring to the amide number in the compound (see Fig. 1). For the smaller dipeptide, Tozer relied on the CASPT2/ANO-“DZP” values of 7.18 eV and 8.07 eV as benchmarks in his original work,⁵⁰ whereas Goerigk proposed reference values of 7.17 and 8.33 eV estimates obtained the CCSDR(3)/*cc-pVTZ* level.

If these values seem numerically consistent, these two transitions are hardly well defined, the mixing of the MO character making unambiguous assignments impossible. As we detail in the SI, this is especially the case for the former $\pi_1 \rightarrow \pi_2^*$ transition that mixes with local excitations. In fact at the same CCSD/*cc-pVTZ* level, Tozer selected the 8.09 eV transition as a CT ES and the 7.35 eV transition as a local ES,⁶⁵ whereas Goerigk made the opposite assignments. Both choices are in fact reasonable based on the selected criteria (see the SI). Due to this confusion, we did only consider the less problematic $n_1 \rightarrow \pi_2^*$ excitation for the dipeptide. For this transition, the CCSDT value is interestingly in-between the CC3 and CCSDT-3 estimates, rather than closer to the CC3 value. As such transition has, chemically speaking, an intermolecular nature, this outcome parallels the finding of Kozma and coworkers who found that CCSDT-3 performs better for intermolecular CTs.⁸⁴ Our TBE/*cc-pVTZ* of 8.15 eV is slightly smaller (larger) than previous CCSDR(3)/TZ (CASPT2/DZ) estimates.

For the β -dipeptide, the identification of the two CT transitions is somehow easier than in the sister compound (see the

SI for details). With the *cc-pVDZ* basis, CCSDT values are roughly midway to CC3 and CCSDT-3. However, the larger size and limited symmetry of β -dipeptide make calculations extremely challenging, and CC3/*cc-pVTZ* calculations were beyond our computational reach. For the $\pi_1 \rightarrow \pi_2^*$ excitation, the CCSDT value is bracketed by the CC3 and CCSDT-3 results, and our TBE of 8.51 eV is slightly below the CCSDR(3) data of Ref. 68, whereas the original CASPT2 transition energy is significantly too small.⁶¹ For the higher lying $n_1 \rightarrow \pi_2^*$ excitation, our best estimate obtained with the same protocol is 8.90 eV, lies below previous estimates.^{61,68}

Given the very large MO mixing with both *cc-pVDZ* and *cc-pVTZ*, we did not attempt to obtain a TBE with diffuse-containing basis sets for these two derivatives.

5.1.9 Hydrogen chloride

HCl is small enough for allowing FCI and CCSDTQ calculations, and both yield a transition energy of 8.10 eV for the hallmark CT excitation with the *cc-pVTZ* basis set. This value is almost perfectly reproduced by both CC3 and CCSDT-3. We could also perform the CCSDTQ/*aug-cc-pVQZ* calculation which returned an excitation energy of 7.88 eV, within 0.02 eV of our previous FCI/CBS value obtained on the same geometry, but with a different computational strategy.⁹³ Given these results, the original CC2/*cc-pVTZ* reference value considered in Tozer’s set (8.23 eV) seems too large by 0.13 eV, whereas the CC3/*aug-cc-pVTZ* value of 7.81 eV used in Ref. 76 could be slightly too low.

5.1.10 Nitroaniline

pNA is a prototypical donor-acceptor system, the potent nitro group allowing an electron-hole separation of the order of 2 Å, about twice the distance determined in the related ABN compound. As in the other nitro-bearing systems discussed below, CCSDT-3 seems to slightly outperform CC3, though the consistency of all CC approaches including triples remains excellent. Our TBEs are 4.57 eV (with *cc-pVTZ*) and 4.39 eV (with *aug-cc-pVQZ*). This latter value is once more exactly equivalent to the one reported by the Klopper group with an extrapolated CC3/*aug-cc-pVTZ* scheme.⁷⁶ Other wavefunction estimates include a 3.80 eV estimate with CASPT2,¹⁷⁶ 4.30 eV with γ -CR-EOMCC(2,3)D/6-31+G(d,p),⁷³ 4.72 eV with EOM-CCSD/*aug-cc-pVDZ*,²⁰² and 4.54 eV with an extrapolated CCSDR(3)/*cc-pVTZ* scheme.⁶⁸

5.1.11 Nitrobenzene

Similarly to the previous case, in nitrobenzene, the pulling group is stronger than in benzonitrile, and the lowest A_1 state gains a significant CT character ($d_{\text{CAM}}^{\text{CT}} = 1.66$ Å, $r_{\text{ADC}}^{\text{eh}} = 1.51$ Å, and $r_{\text{BSE}}^{\text{eh}} = 2.07$ Å). As for the other systems treated herein, the interested reader can find several previous calculations of the ES properties of this substituted system,^{162–164,166,203–205} but to the best of our knowledge, none relied on a CC approach including contributions from the triples. Nevertheless, we wish to point out the joint exhaustive work by the Marian and Drew groups exploring the photo-physics of nitrobenzene,¹⁶⁴ which includes CCSD, NEVPT2, and ADC(3) values for many ESs. While the CCSD transition energy is, as expected too large, there is an excellent agreement between CCSDT and the other CC methods including

iterative triples. The obtained TBEs are likely safe. These TBEs significantly exceed the experimental values, as well as the CASPT2^{162,163} and ADC(3) estimates,¹⁶⁴ but are in good agreement with a recent CR-EOM-CCSD(T)/cc-pVDZ estimate of 5.44 eV.²⁰⁵

5.1.12 Nitrodimethylaniline

This chemical compound is likely one of the strongest donor-acceptor phenyl derivatives that one could envisage. The electron-hole separation in the lowest A_1 ES is enhanced by 0.1–0.3 Å and its energy is downshifted by roughly –0.3 eV as compared to pNA. Otherwise, the methodological trends are exactly the same as in the parent compound, the CCSDT result being bracketed by the CCSDT-3 and CC3 values, and the basis set effects being within expectation for a low-lying ES. Our TBE/*aug-cc-pVQZ* is 0.24 eV larger than the “experimental” λ_{\max} in gas phase,¹⁶⁷ whereas we did not found previous CC estimates for this derivative.

5.1.13 Nitropyridine N-Oxide

This molecule is a solvatochromic probe,²⁰⁶ and its interactions with various solvents were studied in details by various theoretical approaches.¹⁶⁸ Besides it was not investigated theoretically as far as we know, so that this is the first work reporting CC3 and CCSDT-3 transition energies. Unfortunately, the CCSDT/cc-pVDZ corrections failed to properly converge for that specific compound. As a consequence, given the results obtained for the three previous nitro dyes, we went for the CCSDT-3/cc-pVTZ result as reference value. Our TBE/*aug-cc-pVQZ* estimates are 4.10 eV, 0.30 eV above the gas-phase λ_{\max} value estimated in Ref. 168 on the basis of the experimental spectra of Ref. 206. Again, such a difference between a vertical transition energy and an experimental absorption maximum is within expectations for a rigid dye.

5.1.14 N-Phenylpyrrole

PP is a well-known test molecules that is included in many CT sets.^{50,65,68,76,174,207,208} We considered both the planar and twisted (see below) C_{2v} structures here, as in Tozer’s 2012 work.⁶⁵ In the former configuration, the two lowest ESs have a local character, whereas the third ($2 B_2$) and fourth ($3 A_1$) transitions have strong CT characters, with a $r_{\text{ADC}}^{\text{eh}}$ as large as 3.5 Å for the latter. With the cc-pVDZ basis set, the CCSDT energies are bracketed by the CC3 and CCSDT-3 values that are slightly too small and too large respectively. Our TBEs are 5.53 and 6.04 eV with cc-pVTZ, and 5.32 and 5.86 eV with *aug-cc-pVQZ*. The former are close to the extrapolated CCSDR(3)/cc-pVTZ values of Ref. 68, whereas the latter are significantly larger than the extrapolated CC3/*aug-cc-pVTZ* estimates of 5.21 and 5.69 eV given in Ref. 76.

5.1.15 Phthalazine

In this asymmetric bicyclic system, the two lowest ESs, of $n \rightarrow \pi^*$ character, do involve a moderate CT character according to the selected metrics. The data listed in Table 1 show that CC3 and CCSDT do agree very well, whereas the CCSDT-3 transition energies seem too large by approximately 0.1 eV. Our TBE/cc-pVTZ of 3.93 and 4.34 eV are most probably trustworthy for this basis set and decrease only very slightly with the addition of diffuse basis functions. The most refined previous estimates we are aware of are the CC2/*aug-cc-pVDZ* results of Etinski and Marian¹⁶⁹ and the

CASPT2/cc-pVQZ values of Mori and coworkers,¹⁷⁰ and it seems reasonable to state that the TBEs gathered in Table 1 are more accurate. Our vertical energies are, as expected, larger than both experimental peak positions^{171,209} and 0-0 energies.¹⁷²

5.1.16 Quinoxaline

In quinoxaline, we identified three transitions possessing a partial CT character with the selected basis set and models: two $\pi \rightarrow \pi^*$ ESs as well as a higher-lying $n \rightarrow \pi^*$ ES. Confirming the trends obtained above, one notes that the CCSDT excitations energies are roughly in between their CCSDT-3 and CC3 counterparts for the states with a significant electron-hole separation ($r_{\text{ADC}}^{\text{eh}} > 1.5$ Å), but closer to the CC3 results for the transitions with milder CT character ($r_{\text{ADC}}^{\text{eh}} \sim 1.0$ Å). Unexpectedly, the basis set effects seem significantly larger than for phthalazine. For the lowest transition considered, $1B_2$, the present TBE/*aug-cc-pVQZ* of 4.63 eV exceeds significantly the previous CC2/*aug-cc-pVDZ*¹⁶⁹ and CASPT2/cc-pVQZ¹⁷⁰ results. Finally, for the two ESs for which experimental values have been reported,^{171,173} the correct positive difference is once more obtained.

5.1.17 Twisted DMABN and PP

Finally, we consider DMABN and PP in their twisted conformation in which the orthogonality between the NMe₂ or pyrrole group and the phenyl moiety was enforced. The GS structures were optimized in the C_{2v} symmetry. In such conformation, the donor and acceptor units are effectively electronically uncoupled, and one creates two (DMABN) or four (PP) low-lying CT transitions from the nitrogen lone pair (DMABN) or the pyrrole π system (PP) towards the two lowest phenyl π^* orbitals. This also very crudely mimics the possible TICT behavior of these compounds. At the cc-pVDZ level, the CCSDT value falls systematically between the CC3 and CCSDT-3 results, the respective average errors of these two methods being –0.04 eV and +0.07 eV for the six ESs computed on the twisted molecules. In all cases, the basis set effects are rather limited, the cc-pVTZ results being only decreased by ca. –0.10 eV when going to *aug-cc-pVQZ*, except for the A_1 transition of PP for which the basis set effects are slightly larger. For the twisted DMABN our TBE/*aug-cc-pVQZ* values are slightly below the extrapolated CCSD/*aug-cc-pVTZ* data obtained by Tozer.⁶⁵ For twisted PP, the same observation holds and the present TBEs are larger than CASPT2/DZP values obtained two decades ago.¹⁷⁴ In both cases, direct comparisons with experiment, e.g., fluorescence from the TICT structure, remains beyond reach as GS geometries are considered here rather than the ES geometries.

5.2 Benchmarks

5.2.1 Wavefunction and BSE

Having a series TBEs of CCSDT quality at hand, it seems natural to investigate the performances of lower-order approaches. Then, we evaluate here wavefunction-, Green’s function-, and density-based methods. For the two former families we rely on the TBE/cc-pVTZ data as the basis set dependency is similar for these groups of methods. The corresponding results are collected in Table 2. For the vast majority of the cases, the identification of the states was

straightforward for all tested methods, except again for the two peptide derivatives for which a careful inspection of the orbitals/densities was required to reach the correct attribution. At the bottom of Table 2, we also provide statistical quantities obtained by considering these TBEs as reference. We report mean signed error (MSE), mean absolute error (MAE), standard deviation of the errors (SDE), root-mean-square error (RMSE), and maximal positive [Max(+)] and negative [Max(-)] errors. For one transition, our TBE is of CCSDT-3 rather than CCSDT quality, so that the corresponding CCSDT-3 and CC3 results are obviously not included in the statistical analysis (see the footnote in Table 2). Finally, a graphical representation of the error patterns can be found in Fig. 2.

As can be seen in Table 2 and Fig. 2, CIS(D) typically overestimates transition energies, except for the twisted compounds. Hence, this leads to a quite large MSE value of 0.27 eV. The CIS(D) MAE, 0.35 eV, significantly exceeds the 0.22 eV value reported for the local transitions of the very large QUEST database,⁹⁰ hinting that CT states are likely difficult for CIS(D). RPA(D) is somehow superior as its MSE is close to zero, and its MAE is smaller, 0.34 eV, though the differences seem to decrease when the CT character increase. A similar MAE of 0.35 eV was reported with RPA(D) for the valence singlet transitions of Thiel’s set.²¹⁰ EOM-MP2, another “computationally light” method also named CCSD(2) in some works, systematically overshoots the transition energy (except for HCl), the MAE being very large (> 0.50 eV). Note, however, that a quite systematic error pattern is obtained (see Fig. 2), as shown by the very acceptable SDE of 0.19 eV. This typical feature of EOM-MP2 (clear overestimation of the transition energies with a significant increase of the magnitude of the error with system size) was also clearly identified in our previous benchmarks focussing on Rydberg and local transitions.⁹⁰ For their intermolecular CT set, Kozma and coworkers reported a very similar SDE (0.15 eV), but a smaller MSE (0.31 eV) for the same method, a clear overestimation trend being also found.⁸⁴ SOPPA mirrors somehow the behavior of EOM-MP2, with strong underestimations (MSE of -0.62 eV), but in a rather systematic way, so that the SDE is also rather small (0.21 eV). We note that the fact the SOPPA underestimates transition energies was already reported in several benchmarks,^{64,210,211} and is not specific to CT states, though the errors are particularly large here.

As expected,¹³³ CC2 and ADC(2) excitation energies are highly correlated (the R^2 between the two series of transition energies attain 0.995), and we found that the former method has a slight edge in terms of accuracy. For the present CT set, CC2 and ADC(2) are also more accurate than both CIS(D) and EOM-MP2, with MAE of 0.12 eV (CC2) and 0.16 eV [ADC(2)]. Various research groups reported similar average errors for local transitions in molecules of similar sizes.^{90,95,133,134,212–216} Interestingly, when considering only the subset of strong CT ($r_{\text{ADC}}^{\text{eh}} \geq 1.75 \text{ \AA}$), one notes larger errors with significant (and nearly systematic) underestimations leading to negative MSEs of -0.14 eV and -0.19 eV for CC2 and ADC(2), respectively. In other words, both methods tend to undershoot the CT transition energies when the

electron-hole separation becomes sizable. This trend is fully consistent with the investigation of Kozma and coworkers devoted to intermolecular CT ESs:⁸⁴ they reported MSE of -0.36 eV for both methods.

The contrast is clear with CCSD that overestimates quite considerably the transition energies, especially for the strong CT subset with a MSE of +0.37 eV. On the brighter side, CCSD provides quite systematic errors with a SDE of 0.16 eV. These trends are typical of CCSD and were reported in several benchmarks considering local and Rydberg excitations.^{75,90,93,95,134,212,216–221} A MSE of +0.30 eV and a SDE of 0.08 eV have been reported for the 14 intermolecular CT transitions of Ref. 84.

The results obtained with the three CC methods including contributions from the triples are much more satisfying. Indeed, the MAEs are of the order of 0.10 eV (or smaller) and the SDEs are below the 0.05 eV threshold. A near-perfect correlation between the CCSD(T)(a)*, CCSDR(3), and CCSDT-3 transitions is noticeable (R^2 larger than 0.999 for all possible pairs of methods, see also Fig. 2). Comparing the two approaches with perturbative triples, namely, CCSD(T)(a)* and CCSDR(3), one notes very similar deviations, with a slight edge for the second method. Consistently with the results discussed above, CCSDT-3 systematically overestimates the TBEs, whereas CC3 tends to provide slightly too small values. While the sign and magnitude of the differences between the excitation energies obtained with these two CC approaches nicely parallel the findings of Kozma *et al.*,⁸⁴ we find, in contrast to their work, that CC3 is superior as it provides chemically accurate CT excitation energies. This statement holds also when considering only the strong CT subset, and is in line with the results obtained for local and Rydberg transitions of compounds of similar size.^{90,95}

Consistently with our recent investigations,^{90,134} ADC(3) does not significantly improve over ADC(2), as it yields large overestimations for the strong CT subset with a MSE of +0.25 eV, and a MAE of +0.30 eV, together with a significant dispersion (see Fig. 2). Therefore the trends obtained with ADC(3) are opposite to the ones noticed above for ADC(2). The ADC(2.5) approach¹³⁴ — which simply consists in taking the average between the ADC(2) and ADC(3) transition energies — is more accurate than the two other ADC methods with a negligible MSE, a MAE of ca. 0.11 eV, and a SDE of 0.14 eV. These values indicate that ADC(2.5) outperforms all the wavefunction methods tested here sharing the same $O(N^6)$ or a lower $O(N^5)$ computational scaling. These statistical values are totally similar to their local and Rydberg counterparts obtained in the QUEST database (respective MAEs of 0.08 and 0.09 eV),⁹⁰ hinting that ADC(2.5) might be a valuable compromise for many families of transitions.

The BSE/evGW calculations were performed with two very different sets of eigenstates (HF and PBE0) as input. The well-known positive impact of the evGW procedure^{75,76,110,215} undoubtedly emerges in Table 2. Indeed, one obtains a mean absolute deviation (MAD) of 0.33 eV only between the two sets whereas much larger variations would be reached by comparing TD-PBE0 and TD-HF. There is also a strong correlation (R^2 of 0.981) between the two sets of transition energies. In terms of performances, it is clearly

Table 2: CT excitation energies (in eV) obtained with various wavefunction-based methods with the cc-pVTZ basis set. Statistical quantities are reported at the bottom of the Table. For the MSE and MAE, we also provide values obtained for the "strong CT" subgroup, i.e., transitions for which $r_{\text{ADC}}^{\text{eh}} \geq 1.75 \text{ \AA}$.

Molecule	State	TBE	CIS(D)	EOM-MP2	SOPPA	RPA(D)	CC2	CCSD	CCSD(T)(a)*	CCSDR(3)	CCSDT-3	CC3	ADC(2)	ADC(3)	ADC(2.5)	BSE@HF	BSE@PBEO
Aminobenzonitrile	$2A_1(\pi \rightarrow \pi^*)$	5.26	5.57	5.61	4.62	5.21	5.26	5.41	5.32	5.31	5.30	5.25	5.16	5.09	5.12	5.22	5.11
	$2A_1(\pi \rightarrow \pi^*)$	5.87	6.19	6.12	5.27	5.85	5.86	5.99	5.91	5.90	5.90	5.86	5.79	5.74	5.76	5.80	5.64
Aniline	$2A_1(\pi \rightarrow \pi^*)$	3.89	4.14	4.37	3.27	3.93	3.94	4.02	3.98	3.98	3.92	3.88	3.86	3.65	3.75	3.57	3.45
	$2B_2(\pi \rightarrow \pi^*)$	4.55	4.78	5.23	4.05	5.14	4.69	4.82	4.69	4.68	4.61	4.52	4.67	4.45	4.56	4.64	4.40
Benzonitrile	$1A_2(\pi_{\text{CN}} \rightarrow \pi^*)$	7.10	7.85	7.52	6.76	7.69	7.32	7.33	7.17	7.16	7.15	7.08	7.28	6.77	7.03	7.03	6.58
	$1B_2(\pi \rightarrow \pi^*)$	4.37	4.74	5.03	3.79	4.37	4.47	4.63	4.45	4.44	4.40	4.30	4.46	4.04	4.25	4.16	3.89
Benzothiadiazole	$2A_1(\pi \rightarrow \pi^*)$	4.94	5.26	5.33	4.20	4.92	4.85	5.10	5.00	4.99	4.99	4.93	4.73	4.87	4.80	4.97	4.89
	$1B_2(\pi \rightarrow \pi^*)$	4.47	4.67	4.90	3.92	4.22	4.49	4.66	4.54	4.55	4.53	4.48	4.47	4.51	4.49	4.78	4.56
Dimethylaminobenzonitrile	$2A_1(\pi \rightarrow \pi^*)$	5.54	5.95	5.85	4.85	5.63	5.44	5.68	5.59	5.58	5.58	5.53	5.35	5.52	5.44	5.58	5.42
	$2A_1(\pi \rightarrow \pi^*)$	8.15	9.51	9.01	7.48	9.37	7.89	8.92	8.37	8.33	8.31	8.04	7.82	9.22	8.52	9.03	8.59
Dipeptide	$7A'(n_1 \rightarrow \pi_2^*)$	8.51	8.60	9.00	7.96	8.44	8.34	8.90	8.63	8.59 ^a	8.59	8.46 ^b	8.30	8.88	8.59	9.12	8.84
	$7A'(n_1 \rightarrow \pi_2^*)$	8.90	9.71	9.63	8.16	9.67	8.52	9.58	9.14	9.08 ^a	9.02	8.78 ^b	8.45	9.76 ^c	9.10	9.67	9.38
β -Dipeptide	$10A''(n_1 \rightarrow \pi_2^*)$	8.10	8.32	7.98	8.05	8.07	8.28	8.18	8.10	8.10	8.12	8.11	8.30	8.02	8.16	8.41	7.72
	$1\Pi(n \rightarrow \sigma^*)$	4.57	4.75	5.15	3.85	4.36	4.55	4.80	4.67	4.65	4.61	4.51	4.44	4.42	4.43	4.55	4.47
Hydrogen Chloride	$2A_1(\pi \rightarrow \pi^*)$	5.57	5.93	6.11	4.95	5.57	5.63	5.77	5.67	5.64	5.59	5.52	5.55	5.31	5.43	5.47	5.25
	$2A_1(\pi \rightarrow \pi^*)$	4.28	4.44	4.89	3.47	4.06	4.18	4.53	4.39	4.37	4.33	4.22	4.05	4.21	4.13	4.30	4.28
Nitrobenzene	$2A_1(\pi \rightarrow \pi^*)$	4.24	4.26	4.71	2.88	4.52	4.10	4.46	4.31	4.28	4.24 ^d	4.13 ^d	3.62	4.17	3.90	3.85	4.05
	$2B_2(\pi \rightarrow \pi^*)$	5.53	5.98	6.06	5.08	5.62	5.55	5.84	5.62	5.61	5.60	5.50	5.57	5.46	5.52	5.59	5.29
N-Phenylpyrrole	$3A_1(\pi \rightarrow \pi^*)$	6.04	6.35	6.76	5.66	6.23	6.02	6.52	6.18	6.16	6.14	5.97	6.07	6.16	6.11	6.35	6.03
	$1A_2(n \rightarrow \pi^*)$	3.93	4.31	4.47	3.24	3.91	3.78	4.26	4.05	4.04	4.03	3.89	3.79	4.19	3.99	4.39	3.92
Phthalazine	$4A_2(n \rightarrow \pi^*)$	4.34	4.75	4.93	3.61	4.27	4.22	4.64	4.46	4.46	4.43	4.32	4.23	4.49	4.36	4.73	4.28
	$1B_1(n \rightarrow \pi^*)$	4.74	5.17	5.32	4.05	4.92	4.66	5.00	4.82	4.81	4.79	4.69	4.65	4.64	4.64	4.53	4.28
Quinoxaline	$1B_2(\pi \rightarrow \pi^*)$	5.75	5.90	6.36	5.23	5.43	5.83	6.01	5.86	5.86	5.84	5.76	5.82	5.59	5.71	6.83	5.70
	$3A_1(\pi \rightarrow \pi^*)$	6.33	6.81	7.13	5.79	6.45	6.17	6.87	6.50	6.49	6.48	6.26	6.25	6.79	6.52	6.88	6.42
Twisted DMABN	$2B_1(n \rightarrow \pi^*)$	4.17	3.82	4.55	3.36	3.49	3.89	4.41	4.23	4.23	4.25	4.15	3.84	4.56	4.20	4.61	4.32
	$1A_2(n \rightarrow \pi^*)$	4.84	4.38	5.33	4.07	4.12	4.50	5.19	4.91	4.91	4.95	4.81	4.50	5.40	4.95	5.34	5.05
Twisted PP	$2B_2(\pi \rightarrow \pi^*)$	5.73	5.55	6.37	5.23	5.35	5.64	6.10	5.79	5.79	5.80	5.67	5.67	5.87	5.77	6.04	5.65
	$2A_1(\pi \rightarrow \pi^*)$	5.82	6.09	6.41	5.41	5.81	5.78	6.18	5.92	5.91	5.89	5.76	5.82	5.93	5.87	6.07	5.80
MSE	$1A_2(\pi \rightarrow \pi^*)$	6.04	5.90	6.63	5.43	5.56	5.92	6.35	6.11	6.11	6.12	6.01	5.90	6.24	6.07	6.41	6.04
	$1B_1(\pi \rightarrow \pi^*)$	6.28	6.16	6.86	5.69	5.91	6.14	6.61	6.41	6.38	6.36	6.24	6.13	6.57	6.35	6.60	6.27
MSE (strong CT)		0.27	0.53	-0.62	0.01	-0.06	0.30	0.10	0.10	0.08	0.07	-0.04	-0.11	0.09	-0.01	0.22	-0.08
MAE		0.23	0.60	-0.67	-0.02	-0.14	0.37	0.12	0.12	0.10	0.09	-0.05	-0.19	0.25	0.03	0.31	0.03
MAE (strong CT)		0.35	0.53	0.62	0.27	0.12	0.30	0.10	0.08	0.08	0.07	0.04	0.16	0.25	0.11	0.32	0.20
SDE		0.37	0.60	0.67	0.34	0.15	0.37	0.12	0.10	0.09	0.09	0.05	0.19	0.30	0.11	0.38	0.16
RMSE		0.35	0.19	0.21	0.40	0.14	0.16	0.05	0.04	0.04	0.04	0.03	0.18	0.33	0.14	0.35	0.25
Max(+)		0.43	0.56	0.65	0.40	0.15	0.33	0.11	0.09	0.08	0.08	0.05	0.21	0.34	0.13	0.41	0.26
Max(-)		1.36	0.86	-0.05	1.22	0.22	0.77	0.24	0.18	0.16	0.16	0.01	0.20	1.07	0.37	1.08	0.48
		-0.46	-0.12	-1.36	-0.72	-0.38	0.08	0.00	0.00	0.02	0.02	-0.12	-0.62	-0.33	-0.34	-0.39	-0.52

^aBasis set extrapolated CCSDR(3)/cc-pVTZ values from Ref. 68; ^bCC3/cc-pVDZ value corrected by the difference between CCSDT-3/cc-pVTZ and CCSDT-3/cc-pVDZ values; ^cADC(3)/cc-pVDZ value corrected by the difference between ADC(2)/cc-pVTZ and ADC(2)/cc-pVDZ values; ^dNot included in the benchmark statistics.

Table 3: TD-DFT transition energies (in eV) obtained with the *aug-cc-pVQZ* basis set. Statistical quantities are reported at the bottom of the Table. See caption of Table of 2 for more details.

Molecule	State	TBE	B3LYP	PBE0	M06-2X	CAM-B3LYP	LC- ω HPBE	ω B97X	ω B97X-D	M11
Aminobenzonitrile	2 A_1 ($\pi \rightarrow \pi^*$)	5.09	4.87	4.96	5.11	5.06	5.22	5.17	5.10	5.11
Aniline	2 A_1 ($\pi \rightarrow \pi^*$)	5.48	5.24	5.37	5.46	5.42	5.62	5.57	5.49	5.28
Azulene	2 A_1 ($\pi \rightarrow \pi^*$)	3.84	3.60	3.67	3.83	3.72	3.82	3.77	3.72	3.83
	2 B_2 ($\pi \rightarrow \pi^*$)	4.49	4.62	4.71	4.81	4.76	4.85	4.82	4.76	4.84
Benzonitrile	1 A_2 ($\pi_{\text{CN}} \rightarrow \pi^*$)	7.05	6.20	6.29	6.24	6.59	6.85	6.77	6.60	6.75
Benzothiadiazole	1 B_2 ($\pi \rightarrow \pi^*$)	4.28	3.78	3.89	4.19	4.10	4.39	4.28	4.13	4.34
Dimethylaminobenzonitrile	2 A_1 ($\pi \rightarrow \pi^*$)	4.86	4.65	4.74	4.93	4.90	5.07	5.02	4.93	4.99
Dimethylaniline	1 B_2 ($\pi \rightarrow \pi^*$)	4.40	4.41	4.50	4.71	4.67	4.82	4.77	4.67	4.75
	2 A_1 ($\pi \rightarrow \pi^*$)	5.40	5.22	5.31	5.46	5.42	5.57	5.53	5.45	5.47
Hydrogen Chloride	1 Π ($n \rightarrow \sigma^*$)	7.88	7.32	7.57	7.54	7.50	7.94	7.86	7.68	7.34
Nitroaniline	2 A_1 ($\pi \rightarrow \pi^*$)	4.39	3.92	4.08	4.45	4.34	4.68	4.59	4.41	4.59
Nitrobenzene	2 A_1 ($\pi \rightarrow \pi^*$)	5.39	4.72	4.89	5.30	5.11	5.46	5.34	5.17	5.39
Nitrodimethylaniline	2 A_1 ($\pi \rightarrow \pi^*$)	4.13	3.67	3.82	4.23	4.14	4.49	4.41	4.22	4.38
Nitropyridine N-Oxide	2 A_1 ($\pi \rightarrow \pi^*$)	4.10	3.81	3.95	4.22	4.14	4.34	4.30	4.22	4.33
N-Phenylpyrrole	2 B_2 ($\pi \rightarrow \pi^*$)	5.32	4.73	4.86	5.24	5.22	5.66	5.52	5.28	5.44
	3 A_1 ($\pi \rightarrow \pi^*$)	5.86	4.92	5.09	5.83	5.90	6.81	6.52	6.02	6.45
Phthalazine	1 A_2 ($n \rightarrow \pi^*$)	3.91	3.52	3.65	4.02	4.05	4.27	4.25	4.03	4.08
	1 B_1 ($n \rightarrow \pi^*$)	4.31	3.94	4.05	4.24	4.39	4.59	4.57	4.38	4.32
Quinoxaline	1 B_2 ($\pi \rightarrow \pi^*$)	4.63	4.08	4.20	4.61	4.50	4.87	4.73	4.53	4.77
	3 A_1 ($\pi \rightarrow \pi^*$)	5.65	5.70	5.81	5.96	5.91	6.08	6.02	5.93	6.03
	2 B_1 ($n \rightarrow \pi^*$)	6.22	5.69	5.86	6.44	6.46	6.94	6.80	6.44	6.50
Twisted DMABN	1 A_2 ($n \rightarrow \pi^*$)	4.12	3.20	3.34	3.96	3.95	4.38	4.28	3.96	4.11
	1 B_1 ($n \rightarrow \pi^*$)	4.75	3.87	4.04	4.81	4.72	5.38	5.14	4.69	5.03
Twisted PP	2 B_2 ($\pi \rightarrow \pi^*$)	5.58	4.34	4.54	5.29	5.33	6.32	6.05	5.40	5.96
	2 A_1 ($\pi \rightarrow \pi^*$)	5.65	4.43	4.64	5.47	5.54	6.52	6.10	5.65	6.09
	1 A_2 ($\pi \rightarrow \pi^*$)	5.95	4.97	5.17	5.81	5.90	6.56	6.40	6.00	5.78
	1 B_1 ($\pi \rightarrow \pi^*$)	6.17	5.08	5.31	6.08	6.14	6.90	6.70	6.25	
MSE			-0.53	-0.39	-0.02	-0.04	0.35	0.24	0.01	0.12
MSE (strong CT)			-0.73	-0.57	-0.03	-0.02	0.51	0.35	0.03	0.21
MAE			0.55	0.43	0.15	0.14	0.37	0.27	0.13	0.22
MAE (strong CT)			0.73	0.57	0.12	0.10	0.51	0.35	0.10	0.23
SDE			0.38	0.35	0.23	0.18	0.28	0.22	0.17	0.25
RMSE			0.65	0.52	0.22	0.19	0.45	0.32	0.17	0.27
Max(+)			0.13	0.22	0.32	0.27	0.95	0.66	0.28	0.59
Max(-)			-1.24	-1.04	-0.81	-0.46	-0.20	-0.28	-0.45	-0.54

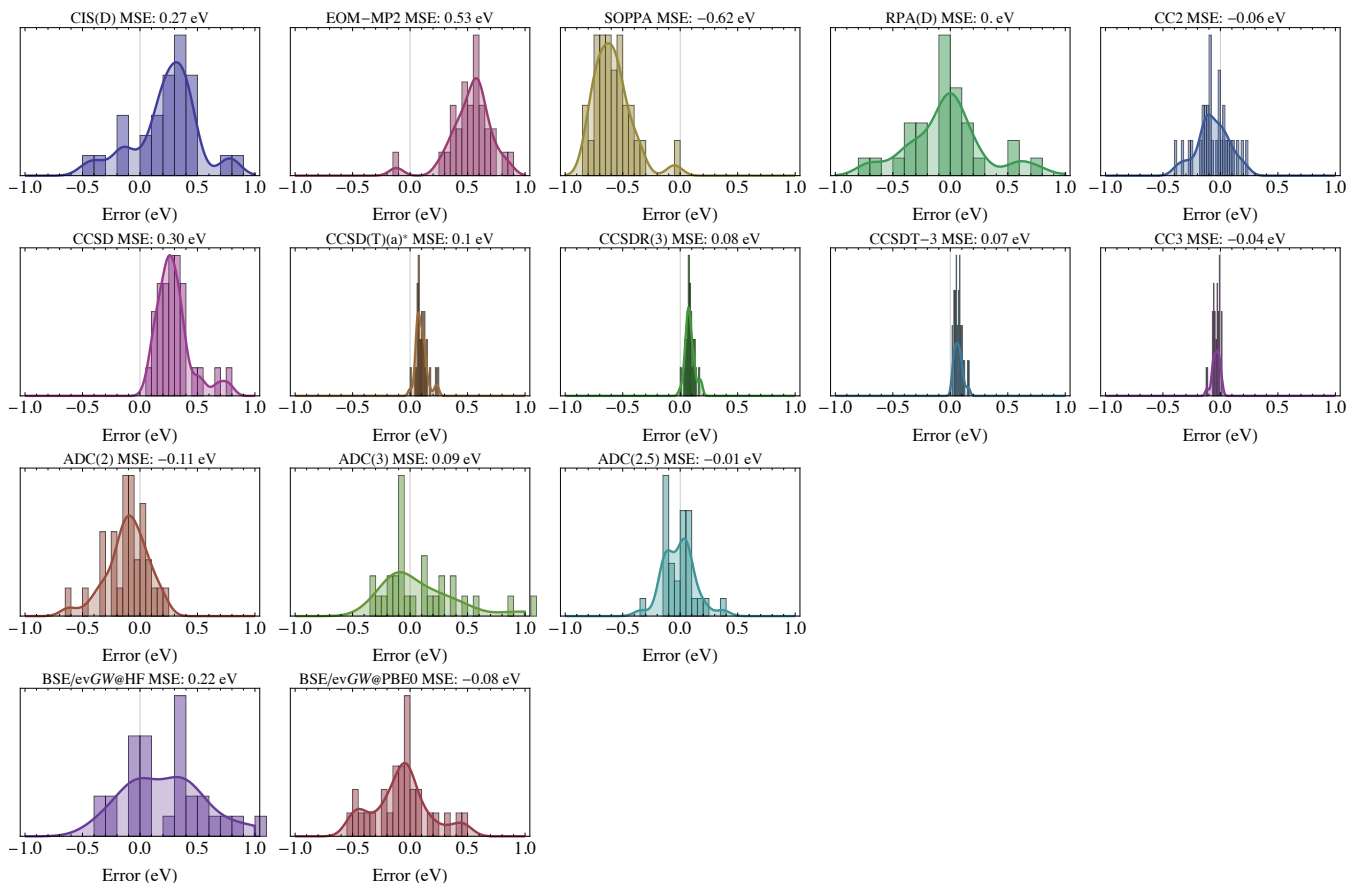


Figure 2: Error patterns against TBE/cc-pVTZ for wavefunction and BSE approaches.

and unsurprisingly more favorable to perform the *evGW* calculations on the basis of KS orbitals. Indeed, for the full set, BSE/*evGW*@PBE0 yields a MAE of 0.20 eV (0.16 eV for the strong CT subset), which is somewhat similar to the ADC(2) performances, though BSE/*evGW*@PBE0 yields less consistent results than these two wavefunction theories with a non-negligible SDE of 0.28 eV. One should recall here that BSE/*evGW*@PBE0 scales as $O(N^4)$, and can be applied to very large systems, so that its global accuracy for the CT transition remains very satisfying in comparison to the associated computational cost. While TD-DFT calculations (see next Subsection) can certainly offer a similar accuracy with proper tuning (range-separation parameter, amount of short/long-range exact exchange) for this specific family of systems, the BSE formalism which relies on the electron-hole screened Coulomb potential instead of the exchange-correlation kernel, allows to tackle with similar accuracy local,^{76,110,222–224} cyanines,²²⁵ and CT excitations. This is an important property in the present case of intramolecular CT excited states that show weak to strong (Frenkel) character. Finally, we note that the quality of the BSE transition energies is also closely related to the ones of the quasiparticles.^{76,222} This also holds at the TD-DFT level.²²⁶

5.2.2 TD-DFT

Let us now turn towards the TD-DFT results listed in Table 3 and displayed in Fig. 3. In this case, we switch to the TBE/*aug-cc-pVQZ* reference data in order to have a fairer comparison between the density-based TD-DFT method and

the wavefunction methods employed to produce these TBEs. Indeed, it is well known that TD-DFT is less sensitive to the basis set size than wavefunction approaches. Therefore, near-CBS limit excitation energies seem to be the only option for a trustworthy comparison between these two families. This choice is however not without consequences. First, TD-DFT calculations become unnecessarily expensive. Second, and more importantly, this extended basis set which contains diffuse basis functions yields significant orbital mixing at the TD-DFT level, blurring the precise nature of the ESs and making the attribution of the various transitions more challenging, a drawback especially marked with LC- ω HPBE and M11.

As expected from previous CT benchmarks,^{5,6,20,50,65} B3LYP and PBE0 tend to underestimate vertical transition energies with errors of the order of -1.0 eV for the pathological cases characterized by a negligible overlap between the occupied and virtual MOs involved in the transition. Likewise, the fact that RSHs tend to be more accurate than B3LYP or PBE0 is no surprise for a benchmark study focussing on CT transitions. Nonetheless, the statistical quantities listed at the bottom of Table 3 show some interesting trends. First, M06-2X, a global hybrid containing 54% of exact exchange, performs well with a MSE of -0.02 eV and a MAE of 0.15 eV (even 0.12 eV for the states in which $r_{\text{ADC}}^{\text{ch}} \geq 1.75$ Å). Although the SDE (0.23 eV) and the largest negative deviation (-0.81 eV for benzonitrile) are sizable, it appears that M06-2X provides quite accurate CT transition energies even

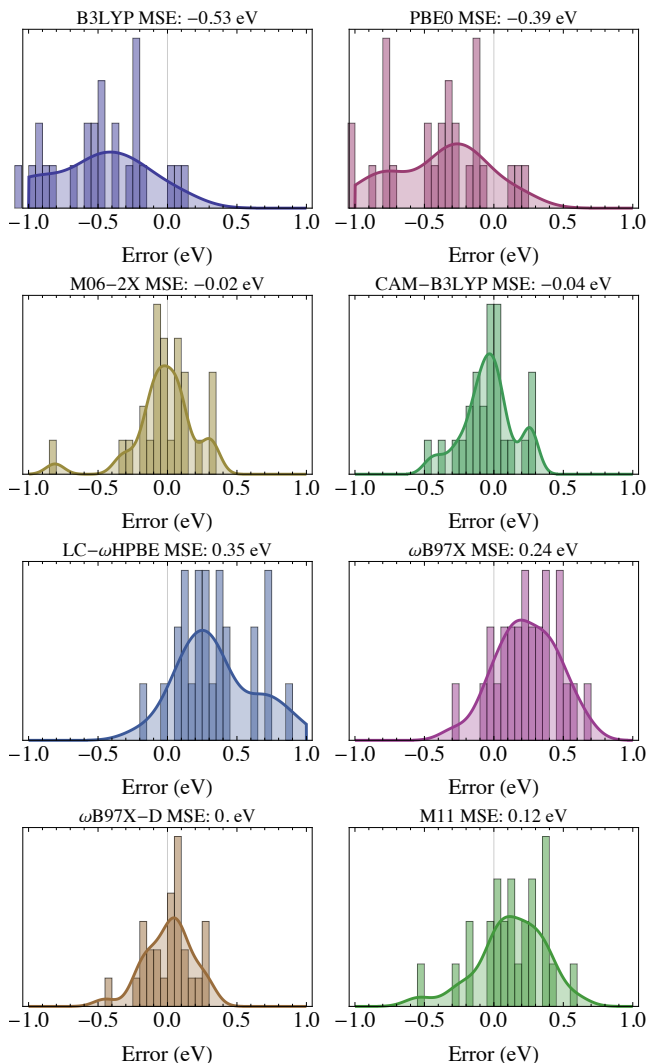


Figure 3: Error patterns against TBE/aug-cc-pVQZ for TD-DFT relying on several XCfs.

for the difficult twisted compounds. Given that the same XCF was shown to be efficient for several other families of transitions,^{215,227–229} M06-2X appears as a handy “Swiss army knife” approach in the TD-DFT framework, though it is not suited for CT excitations where the distance between the hole and the electron is very large.

If one now turns towards the RSH family, one notices that the smallest statistical deviations are obtained with ω B97X-D with MSE close to zero, MAE below 0.15 eV, combined with SDE and RMSE smaller than 0.20 eV. CAM-B3LYP exhibits very similar performances although the MSEs are slightly negative, likely due to the use of “only” 65% of exact exchange at long-range in CAM-B3LYP instead of 100% in ω B97X-D. This induces slight underestimations of the transition energies for the twisted compounds with CAM-B3LYP. The MAE that we determined for CAM-B3LYP (0.14 eV) is significantly smaller than the ones reported in both Refs. 50 (0.27 eV) and 68 (0.46 eV). This might be explained by the fact that the very challenging di- and tri-peptides were included in these previous works. For our test set, the three other RSHs, which include larger shares of exact exchange

tend to be less effective with MAEs of 0.22 eV (M11), 0.27 eV (ω B97X), and 0.37 eV (LC- ω HPBE), and positive MSEs for these three functionals. It is noteworthy that the MAE reported in Ref. 68 for ω B97X is slightly smaller (0.23 eV). Of course, one should keep in mind that the performances of a specific XCF within TD-DFT is very dependent on the nature of the considered transitions. Therefore, the error bars obtained here are likely only relevant for similar intramolecular CT excitations.

6. CONCLUSIONS

We have considered, in a series of π -conjugated compounds, a set of thirty electronic excitation energies presenting a mild to strong intramolecular CT character, the electron-hole separation induced by the electronic transition spanning from 0.83 to 4.35 Å according to an analysis of the ADC(2) transition densities. Using ground state geometries determined at the CC3/cc-pVTZ or CCSD(T)/cc-pVTZ level, we have defined theoretical best estimates (TBEs) for these vertical transition energies by correcting CCSDT/cc-pVDZ values by the difference between CC3/cc-pVTZ and CC3/cc-pVDZ [see Eq. (2)]. These TBEs were further extended to *aug*-cc-pVTZ and *aug*-cc-pVQZ by applying a similar basis set correction approach using CCSDT-3, CCSD and CC2 transition energies [see Eqs. (3) and (4)].

For almost every compounds and states considered here, the present TBEs are the most accurate published to date. Although higher-level calculations (e.g., CCSDTQ) were not technically feasible in the present context, the fact that highly consistent CCSDT-3, CC3, and CCSDT values were almost systematically obtained provides strong confidence in the quality of the present reference data. In more details, for excitations of mild CT character, CC3 and CCSDT transition energies are typically highly similar, as for local valence transitions,⁹⁰ whereas for transitions with more pronounced CT nature, the CCSDT energies are bracketed by CCSDT-3 (high) and CC3 (low). In “pure” intermolecular CT excitation, CCSDT-3 was in fact found to better match CCSDT than CC3.⁸⁴

We hope that the present reference energies will be useful for the electronic structure community developing and assessing new ES theories. As a first step in this direction, we have benchmarked ten popular wavefunction methods, the Bethe-Salpeter equation (BSE) formalism from many-body perturbation theory, as well as TD-DFT with various global and range-separated hybrid functionals. The four CC models including contributions for the triple excitations [i.e., CCSD(T)(a)*, CCSDR(3), CCSDT-3, and CC3] deliver very solid results with small errors and highly-consistent excitation energies. Amongst these approaches, CC3 is the only one providing chemically accurate excitation energies (error below 0.043 eV). The computational cost of these methods is however high. Regarding computationally cheaper methods with a formal $O(N^6)$ scaling with system size, it turns out that (EOM)-JCCSD overestimates the transition energies significantly but with rather systematic errors, whereas ADC(2.5) appears to be a valuable alternative for a similar computational cost. Indeed, ADC(2.5) delivers a MAE of ~ 0.10 eV. Amongst the $O(N^5)$ methods, CC2 is the most effective

with typical underestimations of roughly -0.15 eV but consistent estimates. ADC(2) yields similar, yet slightly less accurate, results than CC2. Amongst the computationally efficient wavefunction schemes, RPA(D) seems to be a reasonable choice. For the most effective $O(N^4)$ approaches allowing calculations on very large systems, one can likely select BSE/evGW@PBE0 which yields consistent estimates for the strong CT transitions, though with a larger dispersion than CC2 or CCSD. With TD-DFT, the most accurate transition energies are produced with (in decreasing order of accuracy) ω B97X-D, CAM-B3LYP, and M06-2X, all three models providing typical errors of approximately 0.15 eV, but again with slightly higher dispersion than most wavefunction methods. The interested reader will find in the SI a Table listing the benchmarked methods, their formal scaling, and the obtained MAEs (Table S7).

The present complementary set of reference energies for CT excited states is currently being merged into the QUEST database of highly-accurate excitation energies which now gathers more than 500 chemically-accurate transition energies.⁹⁰

ACKNOWLEDGEMENTS

XB and DJ thank the ANR for financial support in the framework of the BSE-forces grant. PFL thanks the European Research Council (ERC) under the European Union’s Horizon 2020 research and innovation programme (grant agreement no. 863481) for financial support. DJ is indebted to the CCIPL computational center installed in Nantes for (the always very) generous allocation of computational time. MC and XB acknowledges HPC resources from GENCI-IDRIS Grant 2020-A0090910016.

SUPPORTING INFORMATION AVAILABLE

MO combination and oscillator strengths. Representation of the MOs. Comparison of various CT metrics. Extra details for the dipeptides. Cartesian coordinates for all compounds.

REFERENCES

- (1) Cerón-Carrasco, J. P.; Jacquemin, D.; Laurence, C.; Planchat, A.; Reichardt, C.; Sraïdi, K. Determination of a Solvent Hydrogen-Bond Acidity Scale by Means of the Solvatochromism of Pyridinium-N-phenolate Betaine Dye 30 and PCM-TD-DFT Calculations. *J. Phys. Chem. B* **2014**, *118*, 4605–4614.
- (2) Mulliken, R. S. Molecular Compounds and their Spectra. II. *J. Am. Chem. Soc.* **1952**, *74*, 811–824.
- (3) Dreuw, A.; Head-Gordon, M. Single-Reference *ab initio* Methods for the Calculation of Excited States of Large Molecules. *Chem. Rev.* **2005**, *105*, 4009–4037.
- (4) Maitra, N. T. Charge Transfer in Time-Dependent Density Functional Theory. *Journal of Physics: Condensed Matter* **2017**, *29*, 423001.
- (5) Tozer, D. J. Relationship Between Long-Range Charge-Transfer Excitation Energy Error and Integer Discontinuity in Kohn-Sham Theory. *J. Chem. Phys.* **2003**, *119*, 12697–12699.
- (6) Dreuw, A.; Head-Gordon, M. Failure of Time-Dependent Density Functional Theory for Long-Range Charge-Transfer Excited States: the Zincbacteriochlorin-Bacteriochlorin and Bacteriochlorophyll-Spheroidene Complexes. *J. Am. Chem. Soc.* **2004**, *126*, 4007–4016.
- (7) Perdew, J. P.; Levy, M. Physical Content of the Exact Kohn-Sham Orbital Energies: Band Gaps and Derivative Discontinuities. *Phys. Rev. Lett.* **1983**, *51*, 1884–1887.
- (8) Becke, A. D. Density-Functional Exchange-Energy Approximation with Correct Asymptotic Behavior. *Phys. Rev. A* **1988**, *38*, 3098–3100.
- (9) Lee, C.; Yang, W.; Parr, R. G. Development of the Colle-Salvetti Correlation-Energy Formula Into a Functional of the Electron-Density. *Phys. Rev. B* **1988**, *37*, 785–789.
- (10) Becke, A. D. Density-Functional Thermochemistry. 3. The Role of Exact Exchange. *J. Chem. Phys.* **1993**, *98*, 5648–5652.
- (11) Adamo, C.; Barone, V. Toward Reliable Density Functional Methods Without Adjustable Parameters: the PBE0 Model. *J. Chem. Phys.* **1999**, *110*, 6158–6170.
- (12) Ernzerhof, M.; Scuseria, G. E. Assessment of the Perdew–Burke–Ernzerhof Exchange–Correlation Functional. *J. Chem. Phys.* **1999**, *110*, 5029–5036.
- (13) Savin, A. In *Recent Developments and Applications of Modern Density Functional Theory*; Seminario, J. M., Ed.; Elsevier: Amsterdam, 1996; Chapter 9, pp 327–354.
- (14) Iikura, H.; Tsuneda, T.; Yanai, T.; Hirao, K. A Long-Range Correction Scheme for Generalized-Gradient-Approximation Exchange Functionals. *J. Chem. Phys.* **2001**, *115*, 3540–3544.
- (15) Yanai, T.; Tew, D. P.; Handy, N. C. A New Hybrid Exchange–Correlation Functional Using the Coulomb-Attenuating Method (CAM-B3LYP). *Chem. Phys. Lett.* **2004**, *393*, 51–56.
- (16) Vydrov, O. A.; Scuseria, G. E. Assessment of a Long-Range Corrected Hybrid Functional. *J. Chem. Phys.* **2006**, *125*, 234109.
- (17) Chai, J. D.; Head-Gordon, M. Systematic Optimization of Long-Range Corrected Hybrid Density Functionals. *J. Chem. Phys.* **2008**, *128*, 084106.
- (18) Stein, T.; Kronik, L.; Baer, R. Reliable Prediction of Charge Transfer Excitations in Molecular Complexes Using Time-Dependent Density Functional Theory. *J. Am. Chem. Soc.* **2009**, *131*, 2818–2820.
- (19) Kronik, L.; Stein, T.; Refaely-Ambrason, S.; Baer, R. Excitation Gaps of Finite-Sized Systems from Optimally Tuned Range-Separated Hybrid Functionals. *J. Chem. Theory Comput.* **2012**, *8*, 1515–1531.
- (20) Laurent, A. D.; Jacquemin, D. TD-DFT Benchmarks: A Review. *Int. J. Quantum Chem.* **2013**, *113*, 2019–2039.
- (21) Salpeter, E. E.; Bethe, H. A. A Relativistic Equation for Bound-State Problems. *Phys. Rev.* **1951**, *84*, 1232–1242.

- (22) Hanke, W.; Sham, L. J. Many-Particle Effects in the Optical Excitations of a Semiconductor. *Phys. Rev. Lett.* **1979**, *43*, 387–390.
- (23) Rohlfing, M.; Louie, S. G. Excitonic Effects and the Optical Absorption Spectrum of Hydrogenated Si Clusters. *Phys. Rev. Lett.* **1998**, *80*, 3320–3323.
- (24) Albrecht, S.; Reining, L.; Del Sole, R.; Onida, G. *Ab Initio* Calculation of Excitonic Effects in the Optical Spectra of Semiconductors. *Phys. Rev. Lett.* **1998**, *80*, 4510–4513.
- (25) Benedict, L. X.; Shirley, E. L.; Bohn, R. B. Optical Absorption of Insulators and the Electron-Hole Interaction: An *Ab Initio* Calculation. *Phys. Rev. Lett.* **1998**, *80*, 4514–4517.
- (26) van der Horst, J.-W.; Bobbert, P. A.; Michels, M. A. J.; Brocks, G.; Kelly, P. J. *Ab Initio* Calculation of the Electronic and Optical Excitations in Polythiophene: Effects of Intra- and Interchain Screening. *Phys. Rev. Lett.* **1999**, *83*, 4413–4416.
- (27) Blase, X.; Duchemin, I.; Jacquemin, D. The Bethe-Salpeter Equation in Chemistry: Relations with TD-DFT, Applications and Challenges. *Chem. Soc. Rev.* **2018**, *47*, 1022–1043.
- (28) Blase, X.; Duchemin, I.; Jacquemin, D.; Loos, P. F. The Bethe-Salpeter Formalism: From Physics to Chemistry. *J. Phys. Chem. Lett.* **2020**, *11*, 7371–7382.
- (29) Hedin, L. New Method for Calculating the One-Particle Green’s Function with Application to the Electron-Gas Problem. *Phys. Rev. A* **1965**, *139*, 796–823.
- (30) Strinati, G.; Mattausch, H.; Hanke, W. Dynamical Correlation Effects on the Quasiparticle Bloch States of a Covalent Crystal. *Phys. Rev. Lett.* **1980**, *45*, 290–294.
- (31) Hybertsen, M. S.; Louie, S. G. Electron Correlation in Semiconductors and Insulators: Band Gaps and Quasiparticle Energies. *Phys. Rev. B* **1986**, *34*, 5390–5413.
- (32) Godby, R. W.; Schlüter, M.; Sham, L. J. Self-Energy Operators and Exchange-Correlation Potentials in Semiconductors. *Phys. Rev. B* **1988**, *37*, 10159–10175.
- (33) Onida, G.; Reining, L.; Rubio, A. Electronic Excitations: Density-Functional Versus Many-Body Green’s-Function Approaches. *Rev. Mod. Phys.* **2002**, *74*, 601–659.
- (34) Ping, Y.; Rocca, D.; Galli, G. Electronic excitations in light absorbers for photoelectrochemical energy conversion: first principles calculations based on many body perturbation theory. *Chem. Soc. Rev.* **2013**, *42*, 2437–2469.
- (35) Golze, D.; Dvorak, M.; Rinke, P. The *GW* Compendium: A Practical Guide to Theoretical Photoemission Spectroscopy. *Front. Chem.* **2019**, *7*, 377.
- (36) Blase, X.; Attaccalite, C. Charge-Transfer Excitations in Molecular Donor-Acceptor Complexes Within the Many-Body Bethe-Salpeter Approach. *Appl. Phys. Lett.* **2011**, *99*, 171909.
- (37) Baumeier, B.; Andrienko, D.; Rohlfing, M. Frenkel and Charge-Transfer Excitations in Donor–acceptor Complexes from Many-Body Green’s Functions Theory. *J. Chem. Theory Comput.* **2012**, *8*, 2790–2795.
- (38) Duchemin, I.; Deutsch, T.; Blase, X. Short-Range to Long-Range Charge-Transfer Excitations in the Zincbacteriochlorin-Bacteriochlorin Complex: A Bethe-Salpeter Study. *Phys. Rev. Lett.* **2012**, *109*, 167801.
- (39) Loos, P. F.; Scemama, A.; Jacquemin, D. The Quest for Highly-Accurate Excitation Energies: A Computational Perspective. *J. Phys. Chem. Lett.* **2020**, *11*, 2374–2383.
- (40) Puschnig, P.; Ambrosch-Draxl, C. Suppression of Electron-Hole Correlations in 3D Polymer Materials. *Phys. Rev. Lett.* **2002**, *89*, 056405.
- (41) Tiago, M. L.; Northrup, J. E.; Louie, S. G. *Ab Initio* Calculation of the Electronic and Optical Properties of Solid Pentacene. *Phys. Rev. B* **2003**, *67*, 115212.
- (42) Cudazzo, P.; Gatti, M.; Rubio, A.; Sottile, F. Frenkel versus Charge-Transfer Exciton Dispersion in Molecular Crystals. *Phys. Rev. B* **2013**, *88*, 195152.
- (43) Baumeier, B.; Rohlfing, M.; Andrienko, D. Electronic Excitations in Push-Pull Oligomers and Their Complexes with Fullerene from Many-Body Green’s Functions Theory with Polarizable Embedding. *J. Chem. Theory Comput.* **2014**, *10*, 3104–3110.
- (44) Li, J.; D’Avino, G.; Pershin, A.; Jacquemin, D.; Duchemin, I.; Beljonne, D.; Blase, X. Correlated Electron-Hole Mechanism for Molecular Doping in Organic Semiconductors. *Phys. Rev. Materials* **2017**, *1*, 025602.
- (45) Duchemin, I.; Guido, C. A.; Jacquemin, D.; Blase, X. The Bethe–Salpeter formalism with polarisable continuum embedding: reconciling linear-response and state-specific features. *Chem. Sci.* **2018**, *9*, 4430–4443.
- (46) Trofimov, A.; Schirmer, J. Polarization Propagator Study of Electronic Excitation in key Heterocyclic Molecules I. Pyrrole. *Chem. Phys.* **1997**, *214*, 153–170.
- (47) Dreuw, A.; Wormit, M. The Algebraic Diagrammatic Construction Scheme for the Polarization Propagator for the Calculation of Excited States. *WIREs Comput. Mol. Sci.* **2015**, *5*, 82–95.
- (48) Christiansen, O.; Koch, H.; Jørgensen, P. The Second-Order Approximate Coupled Cluster Singles and Doubles Model CC2. *Chem. Phys. Lett.* **1995**, *243*, 409–418.
- (49) Hättig, C.; Weigend, F. CC2 Excitation Energy Calculations on Large Molecules Using the Resolution of the Identity Approximation. *J. Chem. Phys.* **2000**, *113*, 5154–5161.
- (50) Peach, M. J. G.; Benfield, P.; Helgaker, T.; Tozer, D. J. Excitation Energies in Density Functional Theory: an Evaluation and a Diagnostic Test. *J. Chem. Phys.* **2008**, *128*, 044118.
- (51) Le Bahers, T.; Adamo, C.; Ciofini, I. A Qualitative

- Index of Spatial Extent in Charge-Transfer Excitations. *J. Chem. Theory Comput.* **2011**, *7*, 2498–2506.
- (52) Adamo, C.; Le Bahers, T.; Savarese, M.; Wilbraham, L.; García, G.; Fukuda, R.; Ehara, M.; Rega, N.; Ciofini, I. Exploring Excited States Using Time Dependent Density Functional Theory and Density-Based Indexes. *Coord. Chem. Rev.* **2015**, *304–305*, 166–178.
- (53) Huet, L.; Perfetto, A.; Muniz-Miranda, F.; Campetella, M.; Adamo, C.; Ciofini, I. General Density-Based Index to Analyze Charge Transfer Phenomena: From Models to Butterfly Molecules. *J. Chem. Theory Comput.* **2020**, *16*, 4543–4553.
- (54) Guido, C. A.; Cortona, P.; Mennucci, B.; Adamo, C. On the Metric of Charge Transfer Molecular Excitations: A Simple Chemical Descriptor. *J. Chem. Theory Comput.* **2013**, *9*, 3118–3126.
- (55) Etienne, T.; Assfeld, X.; Monari, A. New Insight into the Topology of Excited States through Detachment/Attachment Density Matrices-Based Centroids of Charge. *J. Chem. Theory Comput.* **2014**, *10*, 3906–3914.
- (56) Plasser, F.; Wormit, M.; Dreuw, A. New Tools for the Systematic Analysis and Visualization of Electronic Excitations. I. Formalism. *J. Chem. Phys.* **2014**, *141*, 024106.
- (57) Plasser, F.; Bäppler, S. A.; Wormit, M.; Dreuw, A. New Tools for the Systematic Analysis and Visualization of Electronic Excitations. II. Applications. *J. Chem. Phys.* **2014**, *141*, 024107.
- (58) Plasser, F. TheoDORE: A Toolbox for a Detailed and Automated Analysis of Electronic Excited State Computations. *J. Chem. Phys.* **2020**, *152*, 084108.
- (59) Andersson, K.; Malmqvist, P. A.; Roos, B. O.; Sadlej, A. J.; Wolinski, K. Second-Order Perturbation Theory With a CASSCF Reference Function. *J. Phys. Chem.* **1990**, *94*, 5483–5488.
- (60) Andersson, K.; Malmqvist, P.-A.; Roos, B. O. Second-Order Perturbation Theory With a Complete Active Space Self-Consistent Field Reference Function. *J. Chem. Phys.* **1992**, *96*, 1218–1226.
- (61) Serrano-Andrés, L.; Fülcher, M. P. Theoretical Study of the Electronic Spectroscopy of Peptides. III. Charge-Transfer Transitions in Polypeptides. *J. Am. Chem. Soc.* **1998**, *120*, 10912–10920.
- (62) Nguyen, K. A.; Day, P. N.; Pachter, R. The Performance and Relationship Among Range-Separated Schemes for Density Functional Theory. *J. Chem. Phys.* **2011**, *135*, 074109.
- (63) Mardirossian, N.; Parkhill, J. A.; Head-Gordon, M. Benchmark Results for Empirical Post-GGA Functionals: Difficult Exchange Problems and Independent Tests. *Phys. Chem. Chem. Phys.* **2011**, *13*, 19325–19337.
- (64) Hedegård, E. D.; Heiden, F.; Knecht, S.; Fromager, E.; Jensen, H. J. A. Assessment of Charge-Transfer Excitations with Time-Dependent, Range-Separated Density Functional Theory Based on Long-Range MP2 and Multiconfigurational Self-Consistent Field Wave Functions. *J. Chem. Phys.* **2013**, *139*, 184308.
- (65) Peach, M. J. G.; Tozer, D. J. Overcoming Low Orbital Overlap and Triplet Instability Problems in TDDFT. *J. Phys. Chem. A* **2012**, *116*, 9783–9789.
- (66) Dev, P.; Agrawal, S.; English, N. J. Determining the Appropriate Exchange-Correlation Functional for Time-Dependent Density Functional Theory Studies of Charge-Transfer Excitations In Organic Dyes. *J. Chem. Phys.* **2012**, *136*, 224301.
- (67) Heßelmann, A. Molecular Excitation Energies from Time-Dependent Density Functional Theory Employing Random-Phase Approximation Hessians with Exact Exchange. *J. Chem. Theory Comput.* **2015**, *11*, 1607–1620.
- (68) Casanova-Páez, M.; Dardis, M. B.; Goerigk, L. ω B2PLYP and ω B2GPPLYP: The First Two Double-Hybrid Density Functionals with Long-Range Correction Optimized for Excitation Energies. *J. Chem. Theory Comput.* **2019**, *15*, 4735–4744.
- (69) Christiansen, O.; Koch, H.; Jørgensen, P. Perturbative Triple Excitation Corrections to Coupled Cluster Singles and Doubles Excitation Energies. *J. Chem. Phys.* **1996**, *105*, 1451–1459.
- (70) Hellweg, A.; Grün, S. A.; Hättig, C. Benchmarking the Performance of Spin-Component Scaled CC2 in Ground and Electronically Excited States. *Phys. Chem. Chem. Phys.* **2008**, *10*, 4119–4127.
- (71) Watts, J. D.; Bartlett, R. J. Economical Triple Excitation Equation-Of-Motion Coupled-Cluster Methods for Excitation Energies. *Chem. Phys. Lett.* **1995**, *233*, 81–87.
- (72) Goerigk, L.; Grimme, S. Assessment of TD-DFT Methods and of Various Spin Scaled CIS_nD and CC2 Versions for the Treatment of Low-Lying Valence Excitations of Large Organic Dyes. *J. Chem. Phys.* **2010**, *132*, 184103.
- (73) Hoyer, C. E.; Ghosh, S.; Truhlar, D. G.; Gagliardi, L. Multiconfiguration Pair-Density Functional Theory is as Accurate as CASPT2 for Electronic Excitation. *J. Phys. Chem. Lett.* **2016**, *7*, 586–591.
- (74) Piecuch, P.; Kucharski, S. A.; Kowalski, K.; Musiał, M. Efficient Computer Implementation of the Renormalized Coupled-Cluster Methods: The R-CCSD[T], R-CCSD(T), CR-CCSD[T], and CR-CCSD(T) Approaches. *Comput. Phys. Commun.* **2002**, *149*, 71–96.
- (75) Jacquemin, D.; Duchemin, I.; Blase, X. Is the Bethe–Salpeter Formalism Accurate for Excitation Energies? Comparisons with TD-DFT, CASPT2, and EOM-CCSD. *J. Phys. Chem. Lett.* **2017**, *8*, 1524–1529.
- (76) Gui, X.; Holzer, C.; Klopper, W. Accuracy Assessment of GW Starting Points for Calculating Molecular Excitation Energies Using the Bethe–Salpeter Formalism. *J. Chem. Theory Comput.* **2018**, *14*, 2127–2136.
- (77) Zhao, Y.; Truhlar, D. G. Benchmark Databases for Nonbonded Interactions and Their Use To Test Density Functional Theory. *J. Chem. Theory Comput.* **2005**, *1*, 415–432.

- (78) Zhao, Y.; Truhlar, D. G. The M06 Suite of Density Functionals for Main Group Thermochemistry, Thermochemical Kinetics, Noncovalent Interactions, Excited States, and Transition Elements: Two New Functionals and Systematic Testing of Four M06-Class Functionals and 12 Other Functionals. *Theor. Chem. Acc.* **2008**, *120*, 215–241.
- (79) Aquino, A. J. A.; Nachtigallova, D.; Hobza, P.; Truhlar, D. G.; Hattig, C.; Lischka, H. The Charge-Transfer States in a Stacked Nucleobase Dimer Complex: A Benchmark Study. *J. Comput. Chem.* **2011**, *32*, 1217–1227.
- (80) Szalay, P. G.; Watson, T.; Perera, A.; Lotrich, V.; Bartlett, R. J. Benchmark Studies on the Building Blocks of DNA. 3. Watson–Crick and Stacked Base Pairs. *J. Phys. Chem. A* **2013**, *117*, 3149–3157.
- (81) Blancafort, L.; Voityuk, A. A. Exciton Delocalization, Charge Transfer, and Electronic Coupling for Singlet Excitation Energy Transfer Between Stacked Nucleobases in DNA: An MS-CASPT2 study. *J. Chem. Phys.* **2014**, *140*, 095102.
- (82) Ghosh, S.; Sonnenberger, A. L.; Hoyer, C. E.; Truhlar, D. G.; Gagliardi, L. Multiconfiguration Pair-Density Functional Theory Outperforms Kohn–Sham Density Functional Theory and Multireference Perturbation Theory for Ground-State and Excited-State Charge Transfer. *J. Chem. Theory Comput.* **2015**, *11*, 3643–3649.
- (83) Ottochian, A.; Morgillo, C.; Ciofini, I.; Frisch, M. J.; Scalmani, G.; Adamo, C. Double Hybrids and Time-Dependent Density Functional Theory: An Implementation and Benchmark on Charge Transfer Excited States. *J. Comput. Chem.* **2020**, *41*, 1242–1251.
- (84) Kozma, B.; Tajti, A.; Demoulin, B.; Izsák, R.; Nooijen, M.; Szalay, P. G. A New Benchmark Set for Excitation Energy of Charge Transfer States: Systematic Investigation of Coupled Cluster Type Methods. *J. Chem. Theory Comput.* **2020**, *16*, 4213–4225.
- (85) Zuluaga, C.; Spata, V. A.; Matsika, S. Benchmarking Quantum Mechanical Methods for the Description of Charge-Transfer States in π -Stacked Nucleobases. *J. Chem. Theory Comput.* **2021**, *17*, 376–387.
- (86) Kowalski, K.; Piecuch, P. The Active-Space Equation-of-Motion Coupled-Cluster Methods for Excited Electronic States: Full EOMCCSDt. *J. Chem. Phys.* **2001**, *115*, 643–651.
- (87) Watts, J. D.; Bartlett, R. J. Iterative and Non-Iterative Triple Excitation Corrections in Coupled-Cluster Methods for Excited Electronic States: the EOM-CCSDT-3 and EOM-CCSD(\bar{T}) Methods. *Chem. Phys. Lett.* **1996**, *258*, 581–588.
- (88) Christiansen, O.; Koch, H.; Jørgensen, P. Response Functions in the CC3 Iterative Triple Excitation Model. *J. Chem. Phys.* **1995**, *103*, 7429–7441.
- (89) Koch, H.; Christiansen, O.; Jørgensen, P.; Olsen, J. Excitation Energies of BH, CH₂ and Ne in Full Configuration Interaction and the Hierarchy CCS, CC2, CCSD and CC3 of Coupled Cluster Models. *Chem. Phys. Lett.* **1995**, *244*, 75–82.
- (90) Véral, M.; Scemama, A.; Caffarel, M.; Lipparini, F.; Boggio-Pasqua, M.; Jacquemin, D.; Loos, P.-F. QUESTDB: a Database of Highly-Accurate Excitation Energies for the Electronic Structure Community. *WIREs Comput. Mol. Sci.* **2021**, *11*, e1517.
- (91) Casanova-Páez, M.; Goerigk, L. Global Double Hybrids do not Work for Charge Transfer: A Comment On “Double Hybrids and Time-Dependent Density Functional Theory: an Implementation and Benchmark on Charge Transfer Excited States”. *J. Comput. Chem.* **2021**, *42*, 528–533.
- (92) Mester, D.; Kállay, M. A Simple Range-Separated Double-Hybrid Density Functional Theory for Excited States. *J. Chem. Theory Comput.* **2021**, *17*, 927–942.
- (93) Loos, P.-F.; Scemama, A.; Blondel, A.; Garniron, Y.; Caffarel, M.; Jacquemin, D. A Mountaineering Strategy to Excited States: Highly-Accurate Reference Energies and Benchmarks. *J. Chem. Theory Comput.* **2018**, *14*, 4360–4379.
- (94) Loos, P.-F.; Boggio-Pasqua, M.; Scemama, A.; Caffarel, M.; Jacquemin, D. Reference Energies for Double Excitations. *J. Chem. Theory Comput.* **2019**, *15*, 1939–1956.
- (95) Loos, P.-F.; Lipparini, F.; Boggio-Pasqua, M.; Scemama, A.; Jacquemin, D. A Mountaineering Strategy to Excited States: Highly-Accurate Energies and Benchmarks for Medium Size Molecules. *J. Chem. Theory Comput.* **2020**, *16*, 1711–1741.
- (96) Loos, P.-F.; Scemama, A.; Boggio-Pasqua, M.; Jacquemin, D. A Mountaineering Strategy to Excited States: Highly-Accurate Energies and Benchmarks for Exotic Molecules and Radicals. *J. Chem. Theory Comput.* **2020**, *16*, 3720–3736.
- (97) Purvis III, G. P.; Bartlett, R. J. A Full Coupled-Cluster Singles and Doubles Model: The Inclusion of Disconnected Triples. *J. Chem. Phys.* **1982**, *76*, 1910–1918.
- (98) Matthews, D. A.; Cheng, L.; Harding, M. E.; Lipparini, F.; Stopkowitz, S.; Jagau, T.-C.; Szalay, P. G.; Gauss, J.; Stanton, J. F. Coupled-Cluster Techniques for Computational Chemistry: The CFOUR Program Package. *J. Chem. Phys.* **2020**, *152*, 214108.
- (99) Loos, P.-F.; Jacquemin, D. Evaluating 0-0 Energies with Theoretical Tools: a Short Review. *ChemPhotoChem* **2019**, *3*, 684–696.
- (100) Peach, M. J. G.; Williamson, M. J.; Tozer, D. J. Influence of Triplet Instabilities in TDDFT. *J. Chem. Theory Comput.* **2011**, *7*, 3578–3585.
- (101) Giner, E.; Scemama, A.; Toulouse, J.; Loos, P. F. Chemically Accurate Excitation Energies With Small Basis Sets. *J. Chem. Phys.* **2019**, *151*, 144118.
- (102) Loos, P. F.; Pradines, B.; Scemama, A.; Toulouse, J.; Giner, E. A Density-Based Basis-Set Correction for Wave Function Theory. *J. Phys. Chem. Lett.* **2019**, *10*, 2931–2937.
- (103) Loos, P. F.; Pradines, B.; Scemama, A.; Giner, E.; Toulouse, J. A Density-Based Basis-Set Incompleteness Correction for GW Methods. *J. Chem. Theory Comput.* **2020**, *16*, 1018–1028.

- (104) Scuseria, G. E.; Scheiner, A. C.; Lee, T. J.; Rice, J. E.; Schaefer, H. F. The Closed-Shell Coupled Cluster Single and Double Excitation (CCSD) Model for the Description of Electron Correlation. A Comparison with Configuration Interaction (CISD) Results. *J. Chem. Phys.* **1987**, *86*, 2881–2890.
- (105) Koch, H.; Jensen, H. J. A.; Jorgensen, P.; Helgaker, T. Excitation Energies from the Coupled Cluster Singles and Doubles Linear Response Function (CCSDLR). Applications to Be, CH⁺, CO, and H₂O. *J. Chem. Phys.* **1990**, *93*, 3345–3350.
- (106) Stanton, J. F.; Bartlett, R. J. The Equation of Motion Coupled-Cluster Method - A Systematic Biorthogonal Approach to Molecular Excitation Energies, Transition-Probabilities, and Excited-State Properties. *J. Chem. Phys.* **1993**, *98*, 7029–7039.
- (107) Stanton, J. F. Many-Body Methods for Excited State Potential Energy Surfaces. I: General Theory of Energy Gradients for the Equation-of-Motion Coupled-Cluster Method. *J. Chem. Phys.* **1993**, *99*, 8840–8847.
- (108) Frisch, M. J.; Trucks, G. W.; Schlegel, H. B.; Scuseria, G. E.; Robb, M. A.; Cheeseman, J. R.; Scalmani, G.; Barone, V.; Petersson, G. A.; Nakatsuji, H.; Li, X.; Caricato, M.; Marenich, A. V.; Bloino, J.; Janesko, B. G.; Gomperts, R.; Mennucci, B.; Hratchian, H. P.; Ortiz, J. V.; Izmaylov, A. F.; Sonnenberg, J. L.; Williams-Young, D.; Ding, F.; Lipparini, F.; Egidi, F.; Goings, J.; Peng, B.; Petrone, A.; Henderson, T.; Ranasinghe, D.; Zakrzewski, V. G.; Gao, J.; Rega, N.; Zheng, G.; Liang, W.; Hada, M.; Ehara, M.; Toyota, K.; Fukuda, R.; Hasegawa, J.; Ishida, M.; Nakajima, T.; Honda, Y.; Kitao, O.; Nakai, H.; Vreven, T.; Throssell, K.; Montgomery, J. A., Jr.; Peralta, J. E.; Ogliaro, F.; Bearpark, M. J.; Heyd, J. J.; Brothers, E. N.; Kudin, K. N.; Staroverov, V. N.; Keith, T. A.; Kobayashi, R.; Normand, J.; Raghavachari, K.; Rendell, A. P.; Burant, J. C.; Iyengar, S. S.; Tomasi, J.; Cossi, M.; Millam, J. M.; Klene, M.; Adamo, C.; Cammi, R.; Ochterski, J. W.; Martin, R. L.; Morokuma, K.; Farkas, O.; Foresman, J. B.; Fox, D. J. Gaussian 16 Revision A.03. 2016; Gaussian Inc. Wallingford CT.
- (109) Krylov, A. I.; Gill, P. M. Q-Chem: an Engine for Innovation. *WIREs Comput. Mol. Sci.* **2013**, *3*, 317–326.
- (110) Jacquemin, D.; Duchemin, I.; Blase, X. Benchmarking the Bethe-Salpeter Formalism on a Standard Organic Molecular Set. *J. Chem. Theory Comput.* **2015**, *11*, 3290–3304.
- (111) Prochnow, E.; Harding, M. E.; Gauss, J. Parallel Calculation of CCSDT and Mk-MRCCSDT Energies. *J. Chem. Theory Comput.* **2010**, *6*, 2339–2347.
- (112) Noga, J.; Bartlett, R. J. The Full CCSDT Model for Molecular Electronic Structure. *J. Chem. Phys.* **1987**, *86*, 7041–7050.
- (113) Scuseria, G. E.; Schaefer, H. F. A New Implementation of the Full CCSDT Model for Molecular Electronic Structure. *Chem. Phys. Lett.* **1988**, *152*, 382–386.
- (114) Kucharski, S. A.; Włoch, M.; Musiał, M.; Bartlett, R. J. Coupled-Cluster Theory for Excited Electronic States: The Full Equation-Of-Motion Coupled-Cluster Single, Double, and Triple Excitation Method. *J. Chem. Phys.* **2001**, *115*, 8263–8266.
- (115) Kowalski, K.; Piecuch, P. Excited-State Potential Energy Curves of CH⁺: a Comparison of the EOM-CCSDt And Full EOMCCSDT Results. *Chem. Phys. Lett.* **2001**, *347*, 237–246.
- (116) Kállay, M.; Gauss, J. Calculation of Excited-State Properties Using General Coupled-Cluster and Configuration-Interaction Models. *J. Chem. Phys.* **2004**, *121*, 9257–9269.
- (117) Balabanov, N. B.; Peterson, K. A. Basis set Limit Electronic Excitation Energies, Ionization Potentials, and Electron Affinities for the 3d Transition Metal Atoms: Coupled Cluster and Multireference Methods. *J. Chem. Phys.* **2006**, *125*, 074110.
- (118) Kamiya, M.; Hirata, S. Higher-Order Equation-of-Motion Coupled-Cluster Methods for Ionization Processes. *J. Chem. Phys.* **2006**, *125*, 074111.
- (119) Watson, M. A.; Chan, G. K.-L. Excited States of Butadiene to Chemical Accuracy: Reconciling Theory and Experiment. *J. Chem. Theory Comput.* **2012**, *8*, 4013–4018.
- (120) Feller, D.; Peterson, K. A.; Davidson, E. R. A Systematic Approach to Vertically Excited States of Ethylene Using Configuration Interaction and Coupled Cluster Techniques. *J. Chem. Phys.* **2014**, *141*, 104302.
- (121) Franke, P. R.; Moore, K. B.; Schaefer, H. F.; Doublerly, G. E. tert-Butyl Peroxy Radical: Ground and First Excited State Energetics and Fundamental Frequencies. *Phys. Chem. Chem. Phys.* **2019**, *21*, 9747–9758.
- (122) Chrayteh, A.; Blondel, A.; Loos, P.-F.; Jacquemin, D. A Mountaineering Strategy to Excited States: Highly-Accurate Oscillator Strengths and Dipole Moments of Small Molecules. *J. Chem. Theory Comput.* **2021**, *17*, 416–438.
- (123) TURBOMOLE V7.3 2018, a development of University of Karlsruhe and Forschungszentrum Karlsruhe GmbH, 1989-2007, TURBOMOLE GmbH, since 2007; available from <http://www.turbomole.com> (accessed 13 June 2016).
- (124) Weigend, F.; Köhn, A.; Hättig, C. Efficient Use of the Correlation Consistent Basis Sets in Resolution of the Identity MP2 Calculations. *J. Chem. Phys.* **2002**, *116*, 3175–3183.
- (125) Head-Gordon, M.; Rico, R. J.; Oumi, M.; Lee, T. J. A Doubles Correction to Electronic Excited States From Configuration Interaction in the Space of Single Substitutions. *Chem. Phys. Lett.* **1994**, *219*, 21–29.
- (126) Head-Gordon, M.; Maurice, D.; Oumi, M. A Perturbative Correction to Restricted Open-Shell Configuration-Interaction with Single Substitutions for Excited-States of Radicals. *Chem. Phys. Lett.* **1995**, *246*, 114–121.
- (127) Stanton, J. F.; Gauss, J. Perturbative Treatment of the Similarity Transformed Hamiltonian in Equation-of-

- Motion Coupled-Cluster Approximations. *J. Chem. Phys.* **1995**, *103*, 1064–1076.
- (128) Nielsen, E. S.; Jorgensen, P.; Oddershede, J. Transition Moments and Dynamic Polarizabilities in a Second Order Polarization Propagator Approach. *J. Chem. Phys.* **1980**, *73*, 6238–6246.
- (129) Bak, K. L.; Koch, H.; Oddershede, J.; Christiansen, O.; Sauer, S. P. A. Atomic Integral Driven Second Order Polarization Propagator Calculations of the Excitation Spectra of Naphthalene and Anthracene. *J. Chem. Phys.* **2000**, *112*, 4173–4185.
- (130) Christiansen, O.; Bak, K. L.; Koch, H.; Sauer, S. P. A. Second-Order Doubles Correction to Excitation Energies in the Random-Phase Approximation. *Chem. Phys. Lett.* **1998**, *284*, 47–55.
- (131) Matthews, D. A.; Stanton, J. F. A new Approach to Approximate Equation-Of-Motion Coupled Cluster with Triple Excitations. *J. Chem. Phys.* **2016**, *145*, 124102.
- (132) Trofimov, A. B.; Stelter, G.; Schirmer, J. Electron Excitation Energies Using a Consistent Third-Order Propagator Approach: Comparison with Full Configuration Interaction and Coupled Cluster Results. *J. Chem. Phys.* **2002**, *117*, 6402–6410.
- (133) Harbach, P. H. P.; Wormit, M.; Dreuw, A. The Third-Order Algebraic Diagrammatic Construction Method (ADC(3)) for the Polarization Propagator for Closed-Shell Molecules: Efficient Implementation and Benchmarking. *J. Chem. Phys.* **2014**, *141*, 064113.
- (134) Loos, P.-F.; Jacquemin, D. Is ADC(3) as Accurate as CC3 for Valence and Rydberg Transition Energies? *J. Phys. Chem. Lett.* **2020**, *11*, 974–980.
- (135) Aidas, K.; Angeli, C.; Bak, K. L.; Bakken, V.; Bast, R.; Boman, L.; Christiansen, O.; Cimiraglia, R.; Coriani, S.; Dahle, P.; Dalskov, E. K.; Ekström, U.; Enevoldsen, T.; Eriksen, J. J.; Ettenhuber, P.; Fernández, B.; Ferrighi, L.; Fliegl, H.; Frediani, L.; Hald, K.; Halkier, A.; Hättig, C.; Heiberg, H.; Helgaker, T.; Hennum, A. C.; Hettema, H.; Hjertenæs, E.; Høst, S.; Hoyvik, I.-M.; Iozzi, M. F.; Jansik, B.; Jensen, H. J. A.; Jonsson, D.; Jørgensen, P.; Kauczor, J.; Kirpekar, S.; Kjærgaard, T.; Klopper, W.; Knecht, S.; Kobayashi, R.; Koch, H.; Kongsted, J.; Krapp, A.; Kristensen, K.; Ligabue, A.; Lutnæs, O. B.; Melo, J. I.; Mikkelsen, K. V.; Myhre, R. H.; Neiss, C.; Nielsen, C. B.; Norman, P.; Olsen, J.; Olsen, J. M. H.; Osted, A.; Packer, M. J.; Pawłowski, F.; Pedersen, T. B.; Provasi, P. F.; Reine, S.; Rinkevicius, Z.; Ruden, T. A.; Ruud, K.; Rybkin, V. V.; Sałek, P.; Samson, C. C. M.; de Merás, A. S.; Saue, T.; Sauer, S. P. A.; Schimmelpfennig, B.; Sneskov, K.; Steindal, A. H.; Sylvester-Hvid, K. O.; Taylor, P. R.; Teale, A. M.; Tellgren, E. I.; Tew, D. P.; Thorvaldsen, A. J.; Thøgersen, L.; Vahtras, O.; Watson, M. A.; Wilson, D. J. D.; Ziolkowski, M.; Ågren, H. The Dalton Quantum Chemistry Program System. *WIREs Comput. Mol. Sci.* **2014**, *4*, 269–284.
- (136) ROWE, D. J. Equations-of-Motion Method and the Extended Shell Model. *Rev. Mod. Phys.* **1968**, *40*, 153–166.
- (137) Kaplan, F.; Harding, M. E.; Seiler, C.; Weigend, F.; Evers, F.; van Setten, M. J. Quasi-Particle Self-Consistent GW for Molecules. *J. Chem. Theory Comput.* **2016**, *12*, 2528–2541.
- (138) Rangel, T.; Hamed, S. M.; Bruneval, F.; Neaton, J. B. Evaluating the GW Approximation with CCSD(T) for Charged Excitations Across the Oligoacenes. *J. Chem. Theory Comput.* **2016**, *12*, 2834–2842.
- (139) Jacquemin, D.; Duchemin, I.; Blase, X. Assessment of the Convergence of Partially Self-Consistent BSE/GW Calculations. *Mol. Phys.* **2015**, *114*, 957–967.
- (140) Stephens, P. J.; Devlin, F. J.; Chabalowski, C. F.; Frisch, M. J. Ab Initio Calculation of Vibrational Absorption and Circular Dichroism Spectra Using Density Functional Force Fields. *J. Phys. Chem.* **1994**, *98*, 11623–11627.
- (141) Barone, V.; Orlandini, L.; Adamo, C. Proton Transfer in Model Hydrogen-Bonded Systems by a Density Functional Approach. *Chem. Phys. Lett.* **1994**, *231*, 295–300.
- (142) Stephens, P. J.; Devlin, F. J.; Frisch, M. J.; Chabalowski, C. F. Ab initio Calculation of Vibrational Absorption and Circular Dichroism Spectra Using Density Functional Force Fields. *J. Phys. Chem.* **1994**, *98*, 11623–11627.
- (143) Henderson, T. M.; Izmaylov, A. F.; Scalmani, G.; Scuseria, G. E. Can Short-Range Hybrids Describe Long-Range-Dependent Properties? *J. Chem. Phys.* **2009**, *131*, 044108.
- (144) Chai, J. D.; Head-Gordon, M. Long-range Corrected Hybrid Density Functionals with Damped Atom-Atom Dispersion Corrections. *Phys. Chem. Chem. Phys.* **2008**, *10*, 6615–6620.
- (145) Peverati, R.; Truhlar, D. Improving the Accuracy of Hybrid Meta-GGA Density Functionals by Range Separation. *J. Phys. Chem. Lett.* **2011**, *2*, 2810–2817.
- (146) Sobolewski, A. L.; Domcke, W. Charge Transfer in Aminobenzonitriles: Do They Twist? *Chem. Phys. Lett.* **1996**, *250*, 428–436.
- (147) Parusel, A. B. J.; Köhler, G.; Nooijen, M. A Coupled-Cluster Analysis of the Electronic Excited States in Aminobenzonitriles. *J. Phys. Chem. A* **1999**, *103*, 4056–4064.
- (148) Zachariasse, K. A.; von der Haar, T.; Hebecker, A.; Leinhos, U.; Kühnle, W. Intramolecular Charge Transfer in Amino-Benzonitriles: Requirements for Dual Fluorescence. *Pure Appl. Chem.* **1993**, *65*, 1745–1750.
- (149) Wang, F.; Neville, S. P.; Wang, R.; Worth, G. A. Quantum Dynamics Study of Photoexcited Aniline. *J. Phys. Chem. A* **2013**, *117*, 7298–7307.
- (150) Honda, Y.; Hada, M.; Ehara, M.; Nakatsuji, H. Excited and Ionized States of Aniline: Symmetry Adapted Cluster Configuration Interaction Theoretical Study. *J. Chem. Phys.* **2002**, *117*, 2045–2052.
- (151) Kimura, K.; Tsubomura, H.; Nagakura, S. The Vacuum Ultraviolet Absorption Spectra of Aniline and

- Some of Its N-Derivatives. *Bull. Chem. Soc. Jpn.* **1964**, *37*, 1336–1346.
- (152) Murakami, A.; Kobayashi, T.; Goldberg, A.; Nakamura, S. CASSCF and CASPT2 Studies on the Structures, Transition Energies, and Dipole Moments of Ground and Excited States for Azulene. *J. Chem. Phys.* **2004**, *120*, 1245–1252.
- (153) Vosskötter, S.; Konieczny, P.; Marian, C. M.; Weinkauff, R. Towards an Understanding of the Singlet–Triplet Splittings in Conjugated Hydrocarbons: Azulene Investigated by Anion Photoelectron Spectroscopy and Theoretical Calculations. *Phys. Chem. Chem. Phys.* **2015**, *17*, 23573–23581.
- (154) Hirata, Y.; Lim, E. C. Radiationless Transitions in Azulene: Evidence for the Ultrafast $S_2 \rightarrow S_0$ Internal Conversion. *J. Chem. Phys.* **1978**, *69*, 3292–3296.
- (155) Fujii, M.; Ebata, T.; Mikami, N.; Ito, M. Electronic Spectra of Jet-Cooled Azulene. *Chem. Phys.* **1983**, *77*, 191–200.
- (156) Lin, T.-S.; Braun, J. R. The Polarized Electronic Spectra and Electric Field Spectra of Benzo-diazoles. II. 2,1,3-Benzothiadiazole. *Chem. Phys.* **1978**, *28*, 379–386.
- (157) Georgieva, I.; Aquino, A. J. A.; Plasser, F.; Trendafilova, N.; Köhn, A.; Lischka, H. Intramolecular Charge-Transfer Excited-State Processes in 4-(N,N-Dimethylamino)benzonitrile: The Role of Twisting and the $\pi\sigma^*$ State. *J. Phys. Chem. A* **2015**, *119*, 6232–6243.
- (158) Mewes, J.-M.; Herbert, J. M.; Dreuw, A. On the Accuracy of the General, State-Specific Polarizable-Continuum Model for the Description of Correlated Ground- and Excited States In Solution. *Phys. Chem. Chem. Phys.* **2017**, *19*, 1644–1654.
- (159) Druzhinin, S. I.; Mayer, P.; Stalke, D.; von Bülow, R.; Noltemeyer, M.; Zachariasse, K. A. Intramolecular Charge Transfer With 1-Tert-Butyl-6-Cyano-1,2,3,4-Tetrahydroquinoline (NTC6) and Other Aminobenzonitriles. A Comparison of Experimental Vapor Phase Spectra and Crystal Structures With Calculations. *J. Am. Chem. Soc.* **2010**, *132*, 7730–7744.
- (160) Fdez. Galván, I.; Elena Martín, M.; Muñoz-Losa, A.; Aguilar, M. A. Solvatochromic Shifts on Absorption and Fluorescence Bands of N,N-Dimethylaniline. *J. Chem. Theory Comput.* **2009**, *5*, 341–349.
- (161) Thompson, J. O. F.; Saalbach, L.; Crane, S. W.; Paterson, M. J.; Townsend, D. Ultraviolet Relaxation Dynamics of Aniline, N,N-Dimethylaniline and 3,5-Dimethylaniline at 250 nm. *J. Chem. Phys.* **2015**, *142*, 114309.
- (162) Kröhl, O.; Malsch, K.; Swiderek, P. The Electronic States of Nitrobenzene: Electron-Energy-Loss Spectroscopy and CASPT2 Calculations. *Phys. Chem. Chem. Phys.* **2000**, *2*, 947–953.
- (163) Giussani, A.; Worth, G. A. Insights into the Complex Photophysics and Photochemistry of the Simplest Nitroaromatic Compound: A CASPT2//CASSCF Study on Nitrobenzene. *J. Chem. Theory Comput.* **2017**, *13*, 2777–2788.
- (164) Mewes, J.-M.; Jovanović, V.; Marian, C. M.; Dreuw, A. On the Molecular Mechanism of Non-Radiative Decay of Nitrobenzene and the Unforeseen Challenges this Simple Molecule Holds for Electronic Structure Theory. *Phys. Chem. Chem. Phys.* **2014**, *16*, 12393–12406.
- (165) Nagakura, S.; Kojima, M.; Maruyama, Y. Electronic Spectra and Electronic Structures of Nitrobenzene and Nitromesitylene. *J. Mol. Spectrosc.* **1964**, *13*, 174–192.
- (166) Krishnakumar, S.; Das, A. K.; Singh, P. J.; Shastri, A.; Rajasekhar, B. Experimental and Computational Studies on the Electronic Excited States of Nitrobenzene. *J. Quant. Spectrosc. Radiat. Transf.* **2016**, *184*, 89–99.
- (167) Laurence, C.; Nicolet, P.; Dalati, M. T.; Abboud, J.-L. M.; Notario, R. The Empirical Treatment of Solvent-Solute Interactions: 15 Years of π^* . *J. Phys. Chem.* **1994**, *98*, 5807–5816.
- (168) Budzák, Š.; Laurent, A. D.; Laurence, C.; Medved', M.; Jacquemin, D. Solvatochromic Shifts in UV–Vis Absorption Spectra: The Challenging Case of 4-Nitropyridine N-Oxide. *J. Chem. Theory Comput.* **2016**, *12*, 1919–1929.
- (169) Etinski, M.; Marian, C. M. A Theoretical Study of Low-Lying Singlet and Triplet Excited States of Quinazoline, Quinoxaline and Phthalazine: Insight into Triplet Formation. *Phys. Chem. Chem. Phys.* **2017**, *19*, 13828–13837.
- (170) Mori, H.; Takeshita, K.; Miyoshi, E.; Ohta, N. Theoretical Quest for Photoconversion Molecules Having Opposite Directions of the Electric Dipole Moment in S_0 and S_1 States. *J. Chem. Phys.* **2009**, *130*, 184311.
- (171) Kaito, A.; Hatano, M. Experimental and Theoretical Studies on the Magnetic Circular Dichroism of Azanaphthalenes. Use of the CNDO/S-CI Approximation. *J. Am. Chem. Soc.* **1978**, *100*, 4037–4044.
- (172) Innes, K.; Ross, I.; Moomaw, W. R. Electronic States of Azabenzenes and Azanaphthalenes: A Revised and Extended Critical Review. *J. Mol. Spectrosc.* **1988**, *132*, 492–544.
- (173) Glass, R. W.; Robertson, L. C.; Merritt, J. A. High-Resolution Electronic Absorption Spectra of Di-azanaphthalenes in the Vapor Phase. *J. Chem. Phys.* **1970**, *53*, 3857–3863.
- (174) Proppe, B.; Merchán, M.; Serrano-Andrés, L. Theoretical Study of the Twisted Intramolecular Charge Transfer in 1-Phenylpyrrole. *J. Phys. Chem. A* **2000**, *104*, 1608–1616.
- (175) Serrano-Andrés, L.; Merchán, M.; Roos, B. O.; Lindh, R. Theoretical Study of the Internal Charge Transfer in Aminobenzonitriles. *J. Am. Chem. Soc.* **1995**, *117*, 3189–3204.
- (176) Serrano-Andrés, L.; Fülcher, M. P.; Karlström, G. Solvent Effects on Electronic Spectra Studied by Multiconfigurational Perturbation Theory. *Int. J. Quantum Chem.* **1997**, *65*, 167–181.
- (177) Gómez, I.; Castro, P. J.; Reguero, M. Insight into the Mechanisms of Luminescence of Aminobenzonitrile and Dimethylaminobenzonitrile in Polar Solvents. An

- ab Initio Study. *J. Phys. Chem. A* **2015**, *119*, 1983–1995.
- (178) Segado, M.; Gómez, I.; Reguero, M. Intramolecular Charge Transfer in Aminobenzonitriles and Tetrafluoro Counterparts: Fluorescence Explained by Competition Between Low-Lying Excited States and Radiationless Deactivation. Part I: A Mechanistic Overview of the Parent System ABN. *Phys. Chem. Chem. Phys.* **2016**, *18*, 6861–6874.
- (179) Castro, P. J.; Perveaux, A.; Lauvergnat, D.; Reguero, M.; Lasorne, B. Ultrafast Internal Conversion in 4-AminoBenzonitrile Occurs Sequentially Along the Seam. *Chem. Phys.* **2018**, *509*, 30–36.
- (180) Dierksen, M.; Grimme, S. A Density Functional Calculation of the Vibronic Structure of Electronic Absorption Spectra. *J. Chem. Phys.* **2004**, *120*, 3544–3554.
- (181) Veys, K.; Escudero, D. Computational Protocol To Predict Anti-Kasha Emissions: The Case of Azulene Derivatives. *J. Phys. Chem. A* **2020**, *124*, 7228–7237.
- (182) Park, S. H.; Roy, A.; Beaupré, S.; Cho, S.; Coates, N.; Moon, J. S.; Moses, D.; Leclerc, M.; Lee, K.; Heeger, A. J. Bulk Heterojunction Solar Cells with Internal Quantum Efficiency Approaching 100%. *Nature Photonics* **2009**, *3*, 297–302.
- (183) Wu, Y.; Zhu, W. Organic Sensitizers from D- π -A to D-A- π -A: Effect of the Internal Electron-Withdrawing Units on Molecular Absorption, Energy Levels and Photovoltaic Performances. *Chem. Soc. Rev.* **2013**, *42*, 2039–2058.
- (184) Mathew, S.; Yella, A.; Gao, P.; Humphry-Baker, R.; Curchod, B. F. E.; Ashari-Astani, N.; Tavernelli, I.; Rothlisberger, U.; Nazeeruddin, M. K.; Grätzel, M. Dye-Sensitized Solar Cells with 13% Efficiency Achieved Through the Molecular Engineering of Porphyrin Sensitizers. *Nature Chem.* **2014**, *6*, 242–247.
- (185) Neto, B. A. D.; Carvalho, P. H. P. R.; Santos, D. C. B. D.; Gatto, C. C.; Ramos, L. M.; Vasconcelos, N. M. d.; Correa, J. R.; Costa, M. B.; de Oliveira, H. C. B.; Silva, R. G. Synthesis, Properties and Highly Selective Mitochondria Staining with Novel, Stable and Superior Benzothiadiazole Fluorescent Probes. *RSC Adv.* **2012**, *2*, 1524–1532.
- (186) Laurent, A. D.; Houari, Y.; Carvalho, P. H. P. R.; Neto, B. A. D.; Jacquemin, D. ESIPT or not ESIPT? Revisiting Recent Results on 2,1,3-benzothiadiazole Under the TD-DFT Light. *RSC Adv.* **2014**, *4*, 14189–14192.
- (187) Roos, B. O.; Andersson, K.; Fulscher, M. P.; Malmqvist, P.-A.; Serrano-Andrés, L. In *Multiconfigurational Perturbation Theory: Applications in Electronic Spectroscopy*; Prigogine, I., Rice, S. A., Eds.; Adv. Chem. Phys.; Wiley, New York, 1996; Vol. 93; pp 219–331.
- (188) Roos, B. O.; Andersson, K.; Fulscher, M. P.; Malmqvist, P.-a.; Serrano-Andres, L.; Pierloot, K.; Merchán, M. *Advances in Chemical Physics*; John Wiley & Sons, Inc., 1997; Vol. 93; Chapter 5, pp 219–331.
- (189) Köhn, A.; Hättig, C. On the Nature of the Low-Lying Singlet States of 4-(Dimethyl-amino)benzonitrile. *J. Am. Chem. Soc.* **2004**, *126*, 7399–7410.
- (190) Grimme, S.; Izgorodina, E. I. Calculation of 0–0 Excitation Energies of Organic Molecules by CIS(D) Quantum Chemical Methods. *Chem. Phys.* **2004**, *305*, 223–230.
- (191) Grimme, S.; Neese, F. Double-Hybrid Density Functional Theory for Excited Electronic States of Molecules. *J. Chem. Phys.* **2007**, *127*, 154116.
- (192) Rhee, Y. M.; Head-Gordon, M. Scaled Second-Order Perturbation Corrections to Configuration Interaction Singles: Efficient and Reliable Excitation Energy Methods. *J. Phys. Chem. A* **2007**, *111*, 5314–5326.
- (193) Wiggins, P.; Gareth Williams, J. A.; Tozer, D. J. Excited State Surfaces in Density Functional Theory: A New Twist on an Old Problem. *J. Chem. Phys.* **2009**, *131*, 091101.
- (194) Rhee, Y. M.; Casanova, D.; Head-Gordon, M. Performance of Quasi-Degenerate Scaled Opposite Spin Perturbation Corrections to Single Excitation Configuration Interaction for Excited State Structures and Excitation Energies with Application to the Stokes Shift of 9-Methyl-9,10-dihydro-9-silaphenanthrene. *J. Phys. Chem. A* **2009**, *113*, 10564–10576.
- (195) Nguyen, K. A.; Day, P. N.; Pachter, R. Analytical Energy Gradients of Coulomb-Attenuated Time-Dependent Density Functional Methods for Excited States. *Int. J. Quantum Chem.* **2010**, *110*, 2247–2255.
- (196) Lunkenheimer, B.; Köhn, A. Solvent Effects on Electronically Excited States Using the Conductor-Like Screening Model and the Second-Order Correlated Method ADC(2). *J. Chem. Theory Comput.* **2013**, *9*, 977–994.
- (197) Yang, Y.; Peng, D.; Lu, J.; Yang, W. Excitation Energies from Particle-Particle Random Phase Approximation: Davidson Algorithm and Benchmark Studies. *J. Chem. Phys.* **2014**, *141*, 124104.
- (198) Mewes, S. A.; Plasser, F.; Krylov, A.; Dreuw, A. Benchmarking Excited-state Calculations Using Exciton Properties. *J. Chem. Theory Comput.* **2018**, *14*, 710–725.
- (199) Caricato, M. CCSD-PCM Excited State Energy Gradients with the Linear Response Singles Approximation to Study the Photochemistry of Molecules in Solution. *ChemPhotoChem* **2019**, *3*, 747–754.
- (200) Rocca, D.; Lu, D.; Galli, G. Ab Initio Calculations of Optical Absorption Spectra: Solution of the Bethe-Salpeter Equation Within Density Matrix Perturbation Theory. *J. Chem. Phys.* **2010**, *133*, 164109.
- (201) Faber, C.; Boulanger, P.; Duchemin, I.; Attaccalite, C.; Blase, X. Many-Body Greens Function GW and Bethe-Salpeter Study of the Optical Excitations in a Paradigmatic Model Dipeptide. *J. Chem. Phys.* **2013**, *139*, 194308.
- (202) Lu, S.-I.; Gao, L.-T. Calculations of Electronic Excitation Energies and Excess Electric Dipole Moments of Solvated p-Nitroaniline with the EOM-CCSD-PCM Method. *J. Phys. Chem. A* **2018**, *122*, 6062–6070.

- (203) André, J. M.; Jacquemin, D.; Perpète, E. A.; Vercauteren, D. P.; Wathélet, V. Assessment of the Accuracy of TD-DFT Absorption Spectra: Substituted Benzenes. *Collect. Czech. Chem. Commun.* **2008**, *73*, 898–908.
- (204) Quenneville, J.; Greenfield, M.; Moore, D. S.; McGrane, S. D.; Scharff, R. J. Quantum Chemistry Studies of Electronically Excited Nitrobenzene, TNA, and TNT. *J. Phys. Chem. A* **2011**, *115*, 12286–12297.
- (205) Schalk, O.; Townsend, D.; Wolf, T. J.; Holland, D. M.; Boguslavskiy, A. E.; Szöri, M.; Stolow, A. Time-Resolved Photoelectron Spectroscopy of Nitrobenzene and its Aldehydes. *Chem. Phys. Lett.* **2018**, *691*, 379–387.
- (206) Lagalante, A. F.; Jacobson, R. J.; Bruno, T. J. UV/Vis Spectroscopic Evaluation of 4-Nitropyridine N-Oxide as a Solvatochromic Indicator for the Hydrogen-Bond Donor Ability of Solvents. *J. Org. Chem.* **1996**, *61*, 6404–6406.
- (207) Xu, X.; Cao, Z.; Zhang, Q. Computational Characterization of Low-Lying States and Intramolecular Charge Transfers in N-Phenylpyrrole and the Planar-Rigidized Fluorazene. *J. Phys. Chem. A* **2006**, *110*, 1740–1748.
- (208) Fdez. Galván, I.; Martín, M. E.; Muñoz-Losa, A.; Sánchez, M. L.; Aguilar, M. A. Solvent Effects on the Structure and Spectroscopy of the Emitting States of 1-Phenylpyrrole. *J. Chem. Theory Comput.* **2011**, *7*, 1850–1857.
- (209) Vasak, M.; Whipple, M. R.; Michl, J. Magnetic Circular Dichroism of Cyclic π -Electron Systems. 7. Aza Analogs of Naphthalene. *J. Am. Chem. Soc.* **1978**, *100*, 6838–6843.
- (210) Sauer, S. P.; Pitzner-Frydendahl, H. F.; Buse, M.; Jensen, H. J. A.; Thiel, W. Performance of SOPPA-Based Methods in the Calculation of Vertical Excitation Energies and Oscillator Strengths. *Mol. Phys.* **2015**, *113*, 2026–2045.
- (211) Haase, P. A. B.; Faber, R.; Provasi, P. F.; Sauer, S. P. A. Noniterative Doubles Corrections to the Random Phase and Higher Random Phase Approximations: Singlet and Triplet Excitation Energies. *J. Comput. Chem.* **2020**, *41*, 43–55.
- (212) Schreiber, M.; Silva-Junior, M. R.; Sauer, S. P. A.; Thiel, W. Benchmarks for Electronically Excited States: CASPT2, CC2, CCSD and CC3. *J. Chem. Phys.* **2008**, *128*, 134110.
- (213) Silva-Junior, M. R.; Schreiber, M.; Sauer, S. P. A.; Thiel, W. Benchmarks of Electronically Excited States: Basis Set Effects Benchmarks of Electronically Excited States: Basis Set Effects on CASPT2 Results. *J. Chem. Phys.* **2010**, *133*, 174318.
- (214) Winter, N. O. C.; Graf, N. K.; Leutwyler, S.; Hättig, C. Benchmarks for 0–0 Transitions of Aromatic Organic Molecules: DFT/B3LYP, ADC(2), CC2, SOS-CC2 and SCS-CC2 Compared to High-resolution Gas-Phase Data. *Phys. Chem. Chem. Phys.* **2013**, *15*, 6623–6630.
- (215) Jacquemin, D.; Duchemin, I.; Blase, X. 0–0 Energies Using Hybrid Schemes: Benchmarks of TD-DFT, CIS(D), ADC(2), CC2, and BSE/GW formalisms for 80 Real-Life Compounds. *J. Chem. Theory Comput.* **2015**, *11*, 5340–5359.
- (216) Kánnár, D.; Tajti, A.; Szalay, P. G. Accuracy of Coupled Cluster Excitation Energies in Diffuse Basis Sets. *J. Chem. Theory Comput.* **2017**, *13*, 202–209.
- (217) Caricato, M.; Trucks, G. W.; Frisch, M. J.; Wiberg, K. B. Electronic Transition Energies: A Study of the Performance of a Large Range of Single Reference Density Functional and Wave Function Methods on Valence and Rydberg States Compared to Experiment. *J. Chem. Theory Comput.* **2010**, *6*, 370–383.
- (218) Watson, T. J.; Lotrich, V. F.; Szalay, P. G.; Perera, A.; Bartlett, R. J. Benchmarking for Perturbative Triple-Excitations in EE-EOM-CC Methods. *J. Phys. Chem. A* **2013**, *117*, 2569–2579.
- (219) Kánnár, D.; Szalay, P. G. Benchmarking Coupled Cluster Methods on Valence Singlet Excited States. *J. Chem. Theory Comput.* **2014**, *10*, 3757–3765.
- (220) Dutta, A. K.; Nooijen, M.; Neese, F.; Izsák, R. Exploring the Accuracy of a Low Scaling Similarity Transformed Equation of Motion Method for Vertical Excitation Energies. *J. Chem. Theory Comput.* **2018**, *14*, 72–91.
- (221) Jacquemin, D. What is the Key for Accurate Absorption and Emission Calculations ? Energy or Geometry ? *J. Chem. Theory Comput.* **2018**, *14*, 1534–1543.
- (222) Bruneval, F.; Hamed, S. M.; Neaton, J. B. A Systematic Benchmark of the Ab Initio Bethe-Salpeter Equation Approach for Low-Lying Optical Excitations of Small Organic Molecules. *J. Chem. Phys.* **2015**, *142*, 244101.
- (223) Nguyen, N. L.; Ma, H.; Govoni, M.; Gygi, F.; Galli, G. Finite-Field Approach to Solving the Bethe-Salpeter Equation. *Phys. Rev. Lett.* **2019**, *122*, 237402.
- (224) Liu, C.; Kloppenburg, J.; Yao, Y.; Ren, X.; Appel, H.; Kanai, Y.; Blum, V. All-Electron ab initio Bethe-Salpeter Equation Approach to Neutral Excitations in Molecules with Numeric Atom-Centered Orbitals. *J. Chem. Phys.* **2020**, *152*, 044105.
- (225) Boulanger, P.; Jacquemin, D.; Duchemin, I.; Blase, X. Fast and Accurate Electronic Excitations in Cyanines with the Many-Body Bethe-Salpeter Approach. *J. Chem. Theory Comput.* **2014**, *10*, 1212–1218.
- (226) Shu, Y.; Truhlar, D. G. Relationships between Orbital Energies, Optical and Fundamental Gaps, and Exciton Shifts in Approximate Density Functional Theory and Quasiparticle Theory. *J. Chem. Theory Comput.* **2020**, *16*, 4337–4350.
- (227) Jacquemin, D.; Zhao, Y.; Valero, R.; Adamo, C.; Ciofini, I.; Truhlar, D. G. Verdict: Time-Dependent Density Functional Theory “Not Guilty” of Large Errors for Cyanines. *J. Chem. Theory Comput.* **2012**, *8*, 1255–1259.
- (228) Leang, S. S.; Zahariev, F.; Gordon, M. S. Benchmarking the Performance of Time-Dependent Density Functional Methods. *J. Chem. Phys.* **2012**, *136*, 104101.

- (229) Isegawa, M.; Peverati, R.; Truhlar, D. G. Performance of Recent and High-Performance Approximate Density Functionals for Time-Dependent Density Functional Theory Calculations of Valence and Rydberg Electronic Transition Energies. *J. Chem. Phys.* **2012**, *137*, 244104.

Graphical TOC Entry

